© 2014. Published by The Company of Biologists Ltd | Journal of Cell Science (2014) 127, 3578–3592 doi:10.1242/jcs.152157

RESEARCH ARTICLE

Aciculin interacts with filamin C and Xin and is essential for myofibril assembly, remodeling and maintenance

Sibylle Molt[1], John B. Bührdel[2], Sergiy Yakovlev[3], Peter Schein[1], Zacharias Orfanos[1], Gregor Kirfel[1], Lilli Winter[4,*], Gerhard Wiche[4], Peter F. M. van der Ven[1], Wolfgang Rottbauer[2], Steffen Just[2], Alexey M. Belkin[3] and Dieter O. Fürst[1,‡]

ABSTRACT

Filamin C (FLNc) and Xin actin-binding repeat-containing proteins (XIRPs) are multi-adaptor proteins that are mainly expressed in cardiac and skeletal muscles and which play important roles in the assembly and repair of myofibrils and their attachment to the membrane. We identified the dystrophin-binding protein aciculin (also known as phosphoglucomutase-like protein 5, PGM5) as a new interaction partner of FLNc and Xin. All three proteins colocalized at intercalated discs of cardiac muscle and myotendinous junctions of skeletal muscle, whereas FLNc and aciculin also colocalized in mature Z-discs. Bimolecular fluorescence complementation experiments in developing cultured mammalian skeletal muscle cells demonstrated that Xin and aciculin also interact in FLNc-containing immature myofibrils and areas of myofibrillar remodeling and repair induced by electrical pulse stimulation (EPS). Fluorescence recovery after photobleaching (FRAP) experiments showed that aciculin is a highly dynamic and mobile protein. Aciculin knockdown in myotubes led to failure in myofibril assembly, alignment and membrane attachment, and a massive reduction in myofibril number. A highly similar phenotype was found upon depletion of aciculin in zebrafish embryos. Our results point to a thus far unappreciated, but essential, function of aciculin in myofibril formation, maintenance and remodeling.

KEY WORDS: Striated muscle, Myofibrillogenesis, Xin actin-binding repeat-containing protein, Phosphoglucomutase, XIRP1, Aciculin, PGM5

INTRODUCTION

The contractile apparatus of striated muscle is a complex macromolecular assembly that is optimized for directed movement. During its development, multiple individual protein components progressively associate to form contractile myofibrils. An equally important task is the maintenance of the structure and functionality of the myofibrils throughout the entire lifespan of an organism. The processes of development, maintenance and, especially, recovery after damage, are still poorly understood, and it is therefore vital to identify the protein components involved and their precise function.

Whereas loss of skeletal muscle fibers resulting from major injuries is compensated for by activation of satellite cells that repair damaged fibers or form new fibers over a period of days, additional and faster mechanisms are required to repair smaller myofibrillar injuries that continuously occur owing to mechanical strain. Such repair zones become evident as regions lacking α-actinin, titin and nebulin, whereas desmin and actin are enriched (Yu et al., 2004; Yu and Thornell, 2002). They are efficiently revealed by staining for filamin C (FLNc) and its ligands Xin and XIRP2 (Eulitz et al., 2013; Kley et al., 2013; Otten et al., 2012; van der Ven et al., 2006). FLNc has also been described as general marker of skeletal muscle damage in numerous neuromuscular diseases (Bönnemann et al., 2003; Sewry et al., 2002; Thompson et al., 2000). Recently, Xin has been identified as a more specific muscle-damage marker localizing in activated satellite cells (Hawke et al., 2007) and in the sarcomeric portion of muscle fibers from patients suffering from myopathies or after eccentric exercise (Nilsson et al., 2013). In healthy tissue, Xin localizes in myotendinous junctions (MTJs) in skeletal muscle and in intercalated discs in the heart (Feng et al., 2013; Otten et al., 2010; van der Ven et al., 2006; Wang et al., 1999). Xin belongs to the family of XIRPs named after their Xin-repeats, peptide motifs which bind actin filaments by coiling around them, similar to nebulin repeats (Cherepanova et al., 2006; Pacholsky et al., 2004). The human Xin-encoding gene (*XIRP1*) gives rise to three products, known as XinA, XinB and XinC. XinA binds the EVH1 domains of Ena/VASP proteins and FLNc, whereas XinB and XinC are splice variants that bind to either EVH1 domains or FLNc, respectively (van der Ven et al., 2006). XinA and XinC also bind the SH3 domain of nebulin and nebulette (Eulitz et al., 2013). The multiplicity of binding partners suggests that Xin acts as a multi-adaptor protein during myofibril development and repair. To obtain a better understanding of these processes at the molecular level, we started to establish the protein interactions of XinB, the most prominent isoform in normal muscle tissue (Gustafson-Wagner et al., 2007; Otten et al., 2010; van der Ven et al., 2006). Considering its proposed function as multi-adaptor protein, we hypothesized that the XinB region C-terminal to the actin-binding repeats functions in establishing multi-protein complexes. Here, we present aciculin as a new interaction partner of this XinB region.

Aciculin, also known as phosphoglucomutase-(PGM)-related protein (PGM-RP) or PGM5, is represented by two closely related 60 kDa and 63 kDa isoforms. It has considerable similarity to PGM1, but lacks enzymatic activity (Belkin et al., 1994).

[1]Institute for Cell Biology, University of Bonn, 53121 Bonn, Germany. [2]Department of Internal Medicine II, University of Ulm, 89081 Ulm, Germany. [3]University of Maryland School of Medicine, Baltimore, MD 21201, USA. [4]Department of Biochemistry and Molecular Cell Biology, Max F. Perutz Laboratories, University of Vienna, 1030 Vienna, Austria.
*Present address: Institute of Neuropathology, University Hospital Erlangen, 91012 Erlangen, Germany.

‡Author for correspondence (dfuerst@uni-bonn.de)

Received 28 February 2014; Accepted 27 May 2014

Journal of Cell Science

Journal of Cell Science (2014) 127, 3578–3592 doi:10.1242/jcs.152157

Aciculin is tightly associated with the actin cytoskeleton and localizes to the ends of stress fibers of cultured cells, epithelial cell–cell contacts, focal adhesions of muscle and some non-muscle cells, and smooth muscle dense bodies (Belkin et al., 1994; Belkin and Burridge, 1995b). In striated muscle, it mainly localizes to the intercalated discs of the heart, and to MTJs and costameres of skeletal muscle (Belkin et al., 1994; Belkin and Burridge, 1994; Belkin and Burridge, 1995a; Belkin and Burridge, 1995b; Koteliansky et al., 1989). Because of its distribution and the subsequent identification of dystrophin as a binding partner (Belkin and Burridge, 1995a; Moiseeva et al., 1996), research on aciculin originally focused on its association with cell–cell and cell–matrix contacts. Given that it is upregulated during muscle cell differentiation, aciculin might also function in muscle development and adaptation (Belkin and Burridge, 1994; Belkin and Burridge, 1995b), for example, following chronic muscle use or disuse (Rezvani et al., 1996). In this report, we analyzed the role of aciculin in myofibril development, maintenance and repair, and found that aciculin is indispensable for myofibril assembly and maintenance in cultured muscle cells and zebrafish embryos.

RESULTS

Identification of aciculin as an interaction partner of Xin

To identify new Xin-interacting proteins, a yeast two-hybrid human heart cDNA library was screened with the C-terminus of XinB (amino acids 756–1121) as bait. Three prey constructs encoding aciculin (UniProt Q15124) or fragments of aciculin, starting from amino acids 250 and 380, respectively, were found. All prey constructs had amino acids 380 to the C-terminus in common. In a reciprocal yeast two-hybrid screen of a human universal cDNA library with full-length aciculin as bait, several Xin fragments were isolated, with a minimal interacting fragment containing amino acids 837–978. Co-immunoprecipitation of XinB with aciculin from a mixture of recombinant proteins confirmed the interaction (Fig. 1A). The C-terminus of XinB contains two amino acid residues lacking in the XinA isoform. To determine whether the interaction depends on these amino acids, we analyzed the interaction of the XinA fragment comprising amino acids 903–1200 with aciculin, and found that aciculin also binds XinA (Fig. 1B).

Our yeast two-hybrid screen indicated that the C-terminal third of aciculin (amino acids 380–567) is sufficient for binding Xin. To further delineate the aciculin-binding motif in Xin, three truncated Xin fragments were tested for binding (Fig. 1C). The fragments comprising amino acids 1–1001 (Fig. 1D) and 1–1057 bound aciculin, whereas the fragment 1–960 did not (data not shown). These data assign the aciculin-binding site within Xin to amino acids 960–978 (Fig. 1C,D). To determine the kinetic parameters of the XinB–aciculin interaction, the association and dissociation of XinB with covalently immobilized aciculin was monitored using surface plasmon resonance (SPR, Fig. 1E). We observed a concentration-dependent and saturable binding of XinB to aciculin with a dissociation constant (K_d) of 369±14 nM (mean±s.e.m.).

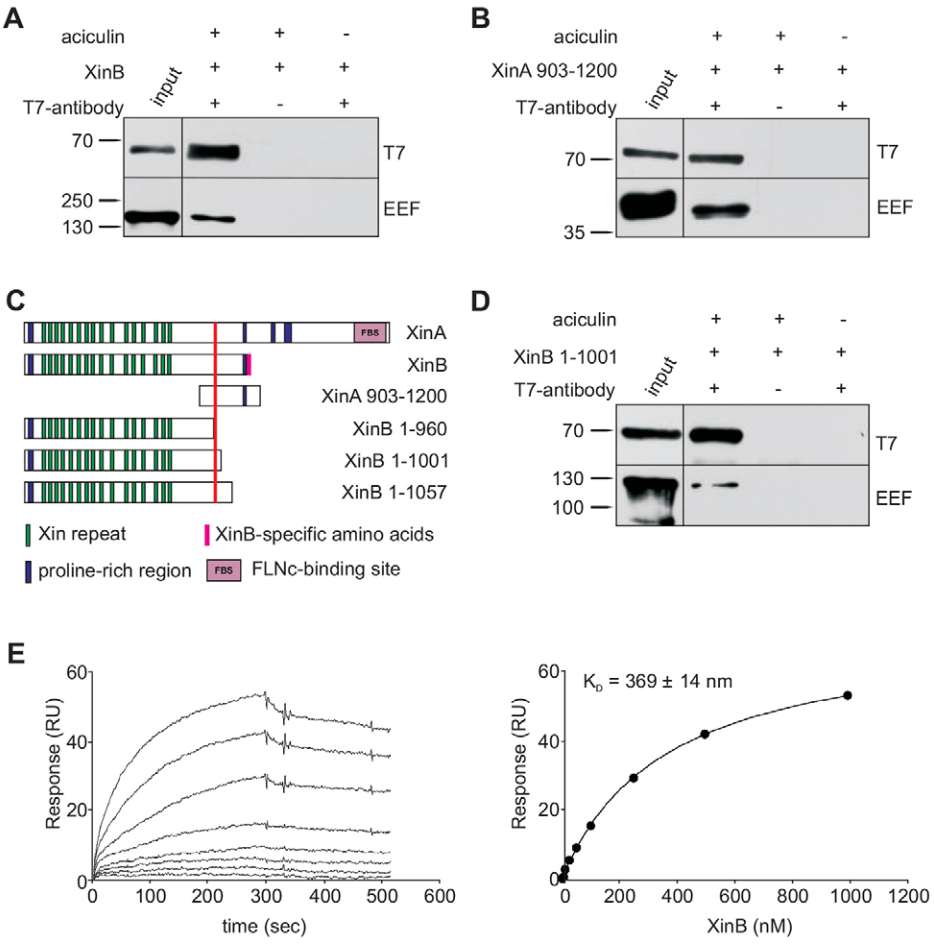

Fig. 1. Aciculin binds Xin *in vitro*. Co-immunoprecipitation analyses confirming binding of aciculin to XinB (A) and the central region of XinA (B), indicating that aciculin does not specifically bind the extreme C-terminal amino acids of XinB. (C) EEF-tagged truncation mutants of XinB used in this study. (D) Constructs 1–1001 and 1–1057 bound T7-tagged aciculin, whereas 1–960 did not. Taken together with data from yeast two-hybrid screens, amino acids 960–978 were identified as the aciculin-binding site (red line in C). Numbers indicate the molecular mass in kDa. (E) Analysis of the XinB–aciculin interaction by SPR (left panel). XinB was added to immobilized aciculin at increasing concentrations and its association and dissociation was monitored. Non-linear regression plot of the response at equilibrium (Req) versus XinB concentration (right panel). The calculated K_d value was 369 nM. RU, response units.

Journal of Cell Science (2014) 127, 3578–3592 doi:10.1242/jcs.152157

Expression and localization of Xin and aciculin in muscle tissue and differentiating skeletal muscle cells

Immunolocalization of aciculin and Xin in cryosections from mouse heart and skeletal muscle tissue indicated that these two proteins colocalized primarily at intercalated discs and MTJs (Fig. 2A). Small amounts of aciculin were also localized in myofibrils, whereas Xin was not. Double-staining for aciculin and a Z-disc epitope of titin showed that aciculin was present at Z-discs (Fig. 2A). Relative expression levels of aciculin and Xin were analyzed in differentiating C2C12 cells by western blotting, revealing that there was expression of aciculin, XinA and XinB from the earliest stages of differentiation. Expression levels of all proteins increased concomitantly, reaching a maximum after 5 days of differentiation (Fig. 2B). Immunolocalization studies of C2C12 myotubes showed colocalization of aciculin and Xin at cortical regions close to the plasma membrane (Fig. 2C, day 1, day 3, arrows) in nascent myofibrils (continuous staining, Fig. 2C, day 4, arrows) and premyofibrils (Z-body staining,

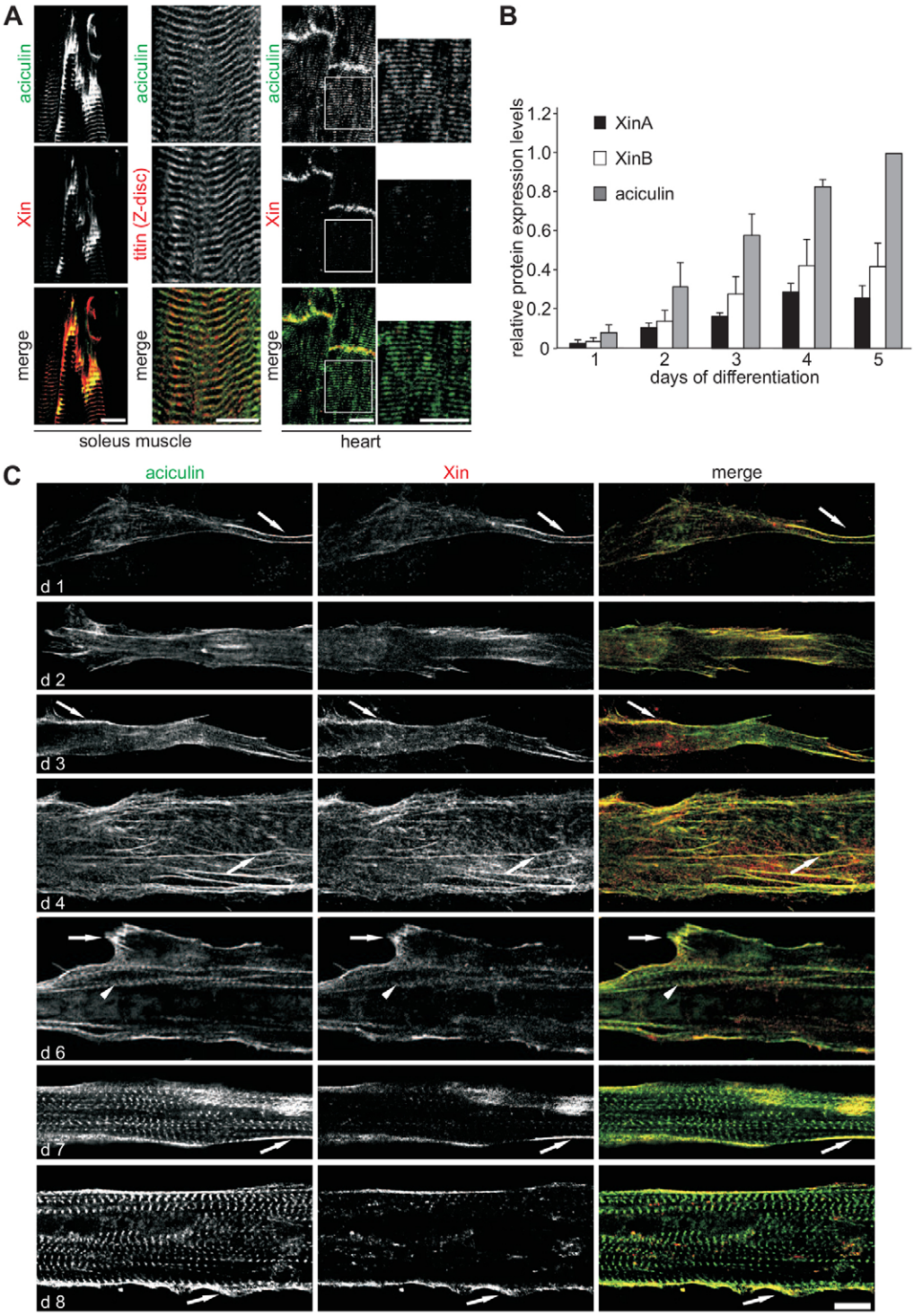

Fig. 2. Xin and aciculin colocalize in adherens junctions and show partial overlap during skeletal muscle cell differentiation. (A) Cryosections of mouse heart and skeletal muscle revealed colocalization of aciculin and Xin in intercalated discs and MTJs, and colocalization of aciculin with a Z-disc epitope of titin. (B) Aciculin and Xin protein levels show a progressive increase during C2C12 differentiation. Data are mean±s.d. of triplicate determinations. (C) Immunostaining differentiating C2C12 cells for aciculin and Xin. Aciculin and Xin colocalize at cortical regions underneath the plasma membrane [arrows, day (d) 1, d3, d7] and in nascent myofibrils (arrow, d4). In mature myotubes aciculin and Xin colocalize in nascent myofibrils and Z-bodies of premyofibrils (arrowheads, d6). In addition, both proteins were prominent in sub-sarcolemmal regions, lamellipodia and filopodia (arrows, d6, d8). Scale bars: 10 μm.

Journal of Cell Science (2014) 127, 3578–3592 doi:10.1242/jcs.152157

Fig. 2C, day 6, arrowheads). Furthermore, both proteins accumulated at cell–substrate adhesions (i.e. at the edges of lamellipodia and filopodia) (Fig. 2C, day 6, day 8, arrows). In mature myotubes, aciculin localized to Z-discs but Xin did not. These findings point to interaction of both proteins at the sarcolemma, in cell–cell and cell–matrix contacts, as well as in immature myofibrils.

FLNc is a myofibrillar interaction partner of aciculin

To identify the binding partner(s) of aciculin in myofibrils, the protein was immunoprecipitated from lysates of differentiated C2C12 cells. Co-precipitated proteins were analyzed for the presence of known Z-disc constituents by immunoblotting. This identified FLNc as a potential binding partner (Fig. 3A). FLNc is a multidomain protein consisting of an N-terminal actin-binding domain followed by 24 immunoglobulin-like domains. Domain 20 contains a unique, most likely unstructured, insertion of 82 amino acids. Subsequent co-immunoprecipitation experiments confirmed direct binding and revealed that domains 18–21 (d18–21) of FLNc are required for binding aciculin (Fig. 3B) because smaller fragments (d18–19, d19–20, d20–21) did not bind. Similarly, FLNc d18–21 without the insertion in d20, and the identical region from the homologous FLNa, also showed no interaction, indicating that the insertion is essential for interaction (data not shown). GST pull-down experiments with immobilized FLNc d18–21 revealed strong binding of FLNc to the N-terminus (amino acids 1–197) of aciculin (Fig. 3G), whereas the C-terminus (amino acids 380–568) of aciculin did not bind (Fig. 3F). Thus, the N-terminus of aciculin is sufficient for binding FLNc, whereas XinB interacts with the C-terminus of aciculin.

Monitoring association and dissociation of aciculin with a covalently immobilized d18–21 FLNc fragment by SPR revealed that binding of aciculin to FLNc was high affinity, concentration dependent and saturable, with a K_d of 51±3 nM (mean±s.e.m.) (Fig. 3C). Solid-phase protein-binding assays were used to define whether XinB and FLNc could simultaneously bind aciculin, thereby forming a ternary XinB–aciculin–FLNc complex

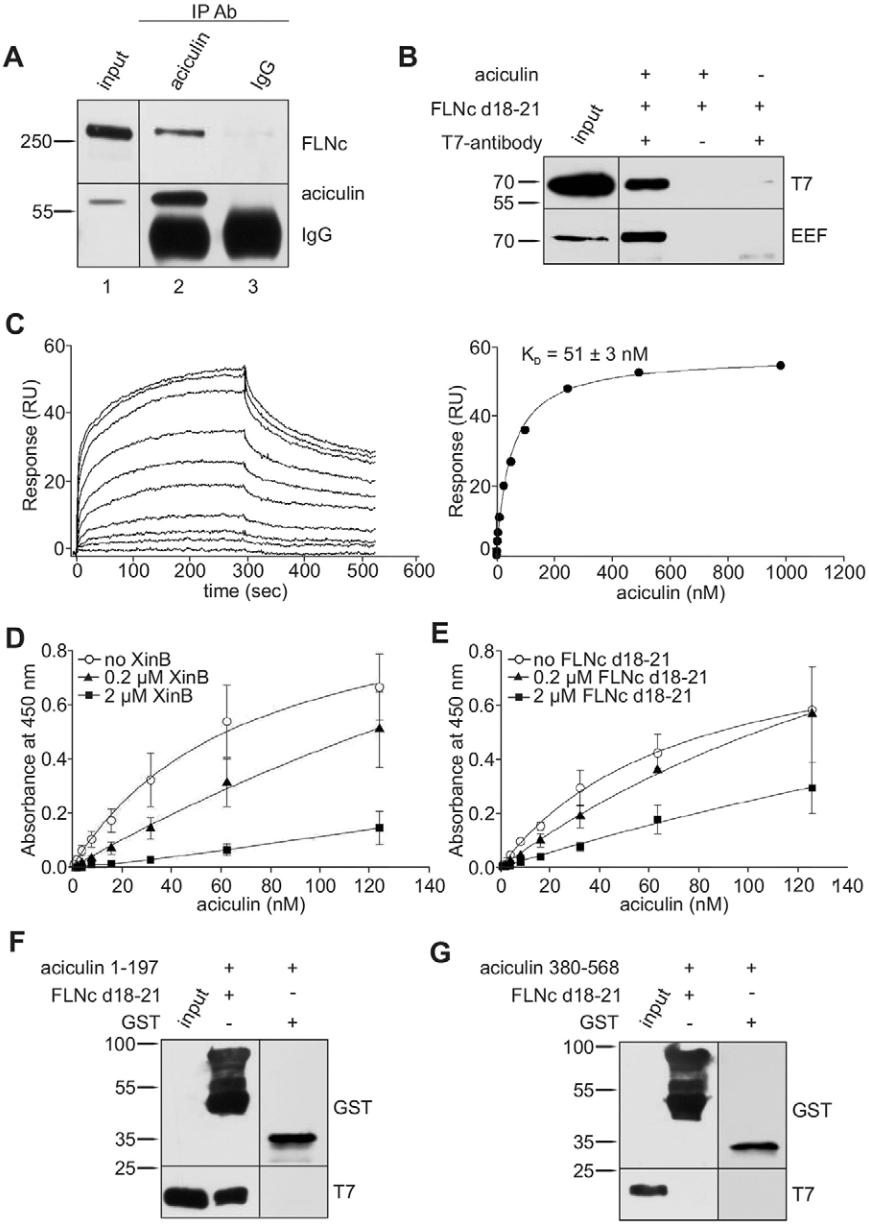

Fig. 3. Aciculin interacts with FLNc. (A) Co-immunoprecipitation of endogenous FLNc and aciculin from differentiated C2C12 cells. Lysate was probed for presence of both proteins (lane 1) and subsequently anti-aciculin antiserum was used to immunoprecipitate (IP) aciculin (lane 2). Preimmune serum (IgG) was used as a negative control (lane 3). Precipitated aciculin (lower panel) and co-precipitated FLNc (upper panel) were detected by immunoblotting. (B) Co-immunoprecipitation analyses confirmed binding of aciculin to FLNc d18–21. (C) Analysis of the aciculin–FLNc interaction by SPR. Left panel, aciculin was added to immobilized FLNc d18–21 at increasing concentrations and its association and dissociation was monitored. Right panel, non-linear regression plot of the response at equilibrium (Req) versus aciculin concentration. The calculated K_d value was 51 nM. RU, response units. (D,E) FLNc d18–21 (D) or XinB (E) were immobilized, and increasing concentrations of aciculin were added either without or with 0.2 μM or 2 μM competing ligand. Aciculin binding was detected by ELISA. Data are means±s.d. of triplicate determinations. (F) GST pull-down assay identified the N-terminus (amino acids 1–197) of aciculin as sufficient for binding FLNc d18–21 (G). The C-terminus (amino acids 380–568) of aciculin did not bind. Numbers indicate molecular mass in kDa.

Journal of Cell Science (2014) 127, 3578–3592 doi:10.1242/jcs.152157

(Fig. 3D,E). Binding of various concentrations of aciculin to FLNc d18–21 (Fig. 3D) or XinB (Fig. 3E) in the absence or presence of 0.2 µM or 2 µM XinB or the FLNc fragment, respectively, showed that the competing ligand substantially reduced the interaction of aciculin with the other ligand. This indicates that XinB and FLNc compete for binding and no ternary complex is formed.

Aciculin exhibits high contraction-dependent mobility

Fluorescence recovery after photobleaching (FRAP) was used to analyze aciculin mobility and dynamics. Defined areas of C2C12 myotubes expressing EGFP–aciculin were photobleached (Fig. 4C,D). In Z-discs and premyofibrils, aciculin recovery followed a biphasic curve with a fast half time of 2.15 and 2.05 s, and slow half time of 55.61 and 61.61 s, respectively (Fig. 4A,B). Mobile fractions were 93%±4 in Z-discs and 94%±6 (mean±s.e.m.) in premyofibrils. This demonstrates that aciculin is a highly mobile protein with extremely high exchange rates in both locations. Similar FRAP analyses were performed in primary skeletal muscle cells from wild-type mice and mice lacking all isoforms of Xin (XinABC$^{-/-}$ mice). No significant differences in recovery times, mobile fractions or localization were detected in Z-discs and premyofibrils, suggesting that aciculin mobility, dynamics and localization are not regulated by its interaction with Xin (supplementary material Fig. S1A–C).

Interestingly, recovery rates (slow half time) in contracting primary cells (22.98 s in Z-discs and 44.93 s in premyofibrils) were significantly faster than those in non-contracting C2C12 cells (supplementary material Table S1). Analysis of aciculin dynamics in C2C12 myotubes that were forced to contract by

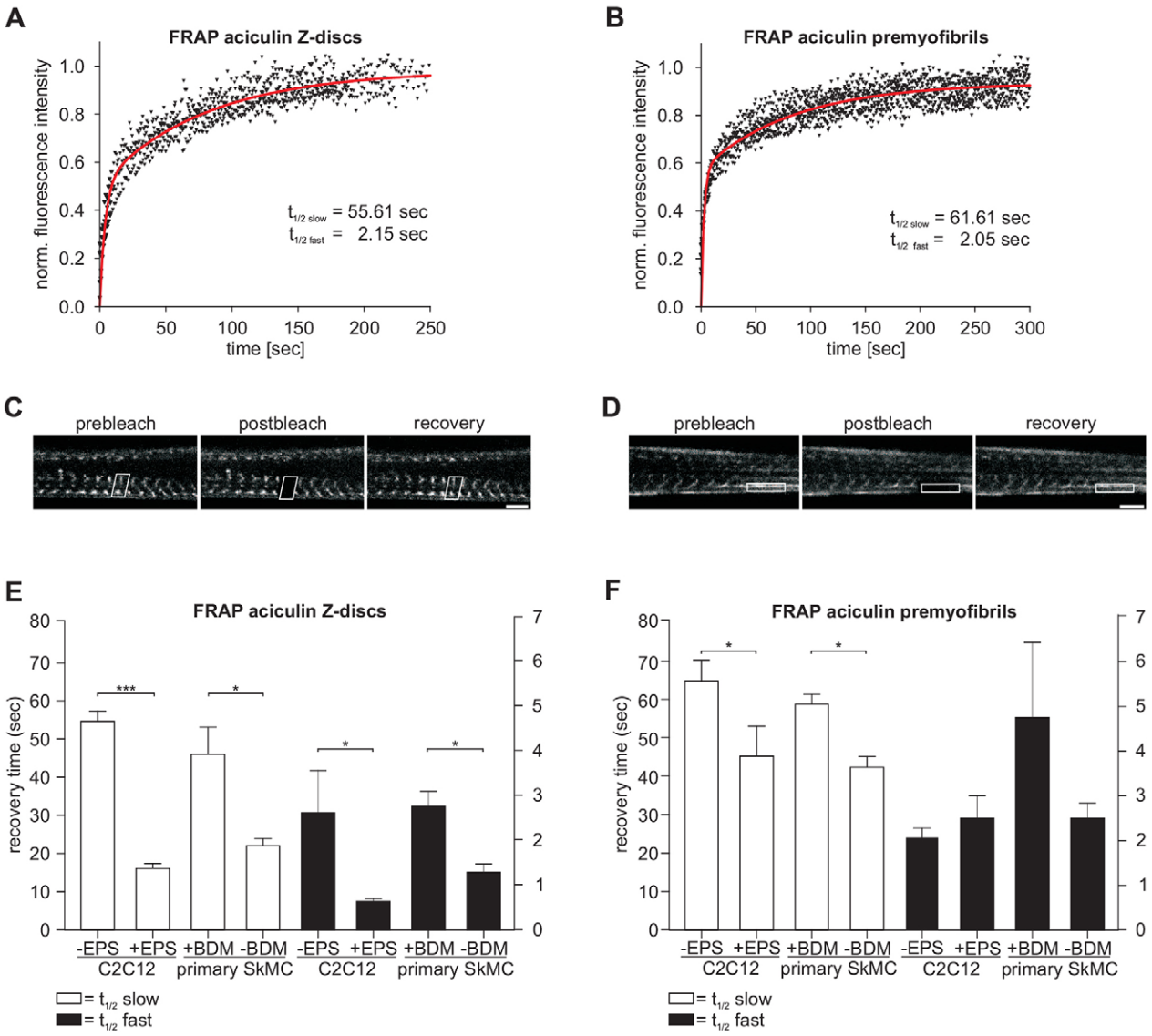

Fig. 4. FRAP studies reveal contraction-dependent high mobility and dynamics of aciculin in C2C12 and primary mouse skeletal muscle cells. (A,B) C2C12 cells transiently transfected with EGFP–aciculin and differentiated for 7 days. The biphasic curve fit (red line) indicates very fast recovery of aciculin in bleached Z-discs and premyofibrils. (C,D) Primary mouse skeletal muscle cells (day 7) before bleaching (prebleach), immediately after bleaching (postbleach) and after recovery (recovery). Bleached regions are framed. Scale bars: 5 µm. (E,F) FRAP studies performed in stimulated (+EPS) and unstimulated (−EPS) C2C12 cells, and in contraction-inhibited (+BDM) and contracting (−BDM) primary skeletal muscle cells (SkMC). Aciculin recovers significantly slower in Z-discs (E) and premyofibrils (F) of non-contracting cells. Bars at the left and right refer to slow and fast half times, respectively. Values are expressed as the mean±s.d. of a minimum of four replicates. *$P<0.05$; ***$P<0.0001$ (Student's *t*-test).

Journal of Cell Science (2014) 127, 3578–3592 doi:10.1242/jcs.152157

electrical pulse stimulation (EPS) and in primary skeletal muscle cells where contraction was inhibited by addition of 2,3-butanedione monoxine (BDM) to the culture medium, confirmed that the recovery times of both cell types were significantly faster in contracting myotubes. The effect was more pronounced in Z-discs than in premyofibrils (Fig. 4E,F). These findings demonstrate that aciculin dynamics are enhanced by contraction.

Aciculin interacts with Xin in areas of myofibrillar damage and remodeling in skeletal muscle cells

FLNc and Xin colocalize in regions of myofibrillar reorganization that appear in typical longitudinal structures spanning two neighboring or several subsequent Z-discs (Eulitz et al., 2013). Triple-immunostaining of cryosections of mouse skeletal muscle tissue for aciculin, Xin and FLNc showed that all areas of myofibril remodeling also contained aciculin (Fig. 5A,B).

Staining differentiating C2C12 cells for aciculin and Xin showed their colocalization in nascent myofibrils and premyofibrils (Fig. 2C). Areas of remodeling as found in myotubes derived from H-2Kb-tsA58 transgenic mice, from which immortalized cell lines can be derived (Eulitz et al., 2013; Morgan et al., 1994), were not observed (Fig. 5C). Application of EPS on C2C12 myotubes induced remodeling and yielded aciculin- and Xin-containing structures closely resembling the longitudinal structures observed in skeletal muscle tissue and

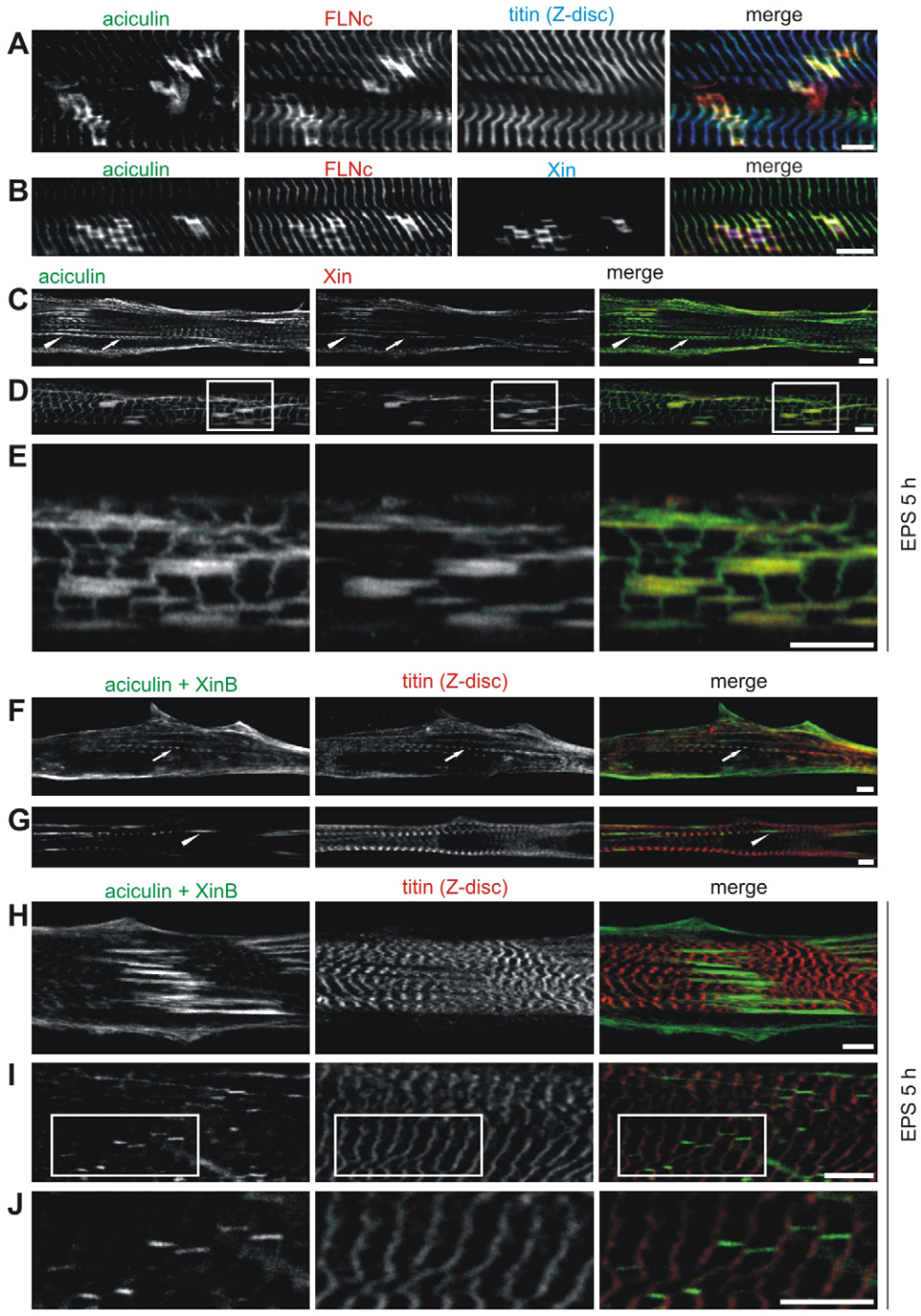

Fig. 5. Aciculin interacts with Xin and FLNc in areas of myofibrillar damage and reorganization in muscle cells. Aciculin colocalizes with FLNc (A) and Xin (B) in longitudinal structures spanning one or several Z-discs in mouse skeletal muscle sections. (C) In C2C12 myotubes, aciculin colocalizes with Xin in nascent myofibrils (arrowhead) and in Z-bodies of premyofibrils (arrow). (D) EPS induces Xin and aciculin colocalization in regions of myofibril reorganization. Boxed areas are enlarged in E. (F,G) BiFC confirms the interaction between XinB–Venus1 and Venus2–aciculin in Z-bodies (arrows) and nascent myofibrils (arrowheads). (H–J) In EPS-treated C2C12 myotubes, XinB–Venus1 and Venus2–aciculin interact in regions of myofibril reorganization. Boxed areas in I are enlarged in J. Scale bars: 5 μm.

Journal of Cell Science (2014) 127, 3578–3592 doi:10.1242/jcs.152157

contracting H-2Kb-tsA58 myotubes (Fig. 5D,E). These observations support the hypothesis that aciculin interacts with Xin during myofibril reorganization after damage.

To investigate when and where XinB and aciculin interact in cells, bimolecular fluorescence complementation (BiFC) assays were performed on C2C12 myotubes expressing XinB–Venus1N and Venus2C–aciculin. Venus1 and Venus2 only form a functional fluorescent complex when they associate, hence this fluorescence is indicative of an interaction. In unstimulated cells, interaction between aciculin and XinB was observed in regions similar to those shown to contain both proteins by immunostaining untransfected myotubes (Fig. 5F,G). Upon EPS for 5 h, however, a BiFC signal was observed in longitudinal structures bridging two or several Z-discs (Fig. 5H–J), a location where GFP–XinB and GFP–aciculin are also observed upon their individual expression (supplementary material Fig. S2A). XinB–Venus1N and Venus2C–aciculin gave a fusion peptide of the expected molecular mass and with expression levels similar to the endogenous proteins (supplementary material Fig. S2C), and coexpression of XinB and aciculin with the corresponding non-fused Venus fragment yielded no fluorescent signal, emphasizing the specificity of this approach (supplementary material Fig. S2B). These findings point to a role for aciculin and Xin during myofibrillar remodeling and repair, and confirm the interaction of aciculin and XinB in cortical regions of myotubes.

Aciculin knockdown leads to severe myofibrillar defects in skeletal muscle cells

The role of aciculin in muscle structure and function was further investigated by the generation of a stable immortalized mouse myoblast (IMM) cell line in which expression of aciculin had been reduced using lentivirus expressing aciculin short hairpin RNA (shRNA) and a control cell line using scrambled-shRNA-expressing virus. Knockdown cells proliferated and fused normally. Quantitative western blot analysis revealed similar aciculin expression levels at early developmental stages but an ~60% reduction in knockdown cells after 4 days of differentiation (Fig. 6A). Aciculin knockdown induced a slight, but not significant, upregulation of XinA, XinB and FLNc, whereas levels of α-actinin, myosin heavy chain and myomesin were significantly decreased (~50%, 35% and 25%, respectively; Fig. 6B). Quantitative RT-PCR analysis confirmed downregulation of mRNA encoding aciculin and α-actinin2 (Fig. 6C). The expression of other mRNAs analyzed, including that encoding the homologous PGM1, were essentially unaffected (Fig. 6C). Immunostaining for α-actinin, myomesin, FLNc and Xin revealed highly ordered mature myofibrils in control cells. In contrast, aciculin-knockdown cells contained fewer myofibrils that were misaligned and showed only a rudimentary sarcomeric organization. Notably, FLNc was no longer found in the remaining Z-discs (Fig. 6D, arrows). Transient transfection of the aciculin-knockdown cells with EGFP-tagged human aciculin, the expression of which is not silenced by the applied shRNA, rescued the phenotype. Staining for a Z-disc epitope of titin revealed recovery of sarcomeric organization (Fig. 6E), indicating that an off-target effect of the shRNA can be excluded.

Knockdown of aciculin leads to myopathy *in vivo*

To investigate the function of aciculin in zebrafish (*Danio rerio*), we first identified the orthologous gene (*pgm5*, Ensembl ID: ENSDARG00000060745) and protein. Zebrafish aciculin has an amino acid identity of 77% to human aciculin (supplementary material Fig. S3A). *pgm5* mRNA became detectable in developing somites at the four-somite stage. Before the 18-somite stage, expression was largely restricted to these structures. At 24 h post-fertilization (hpf), *pgm5* was highly expressed in caudal developing somites, whereas expression was reduced in developmentally older cranial somites (Fig. 7A–C). This suggests that aciculin is involved in myofibril assembly, which primarily occurs in the less-developed somites. Owing to the lack of antibodies recognizing zebrafish aciculin in immunofluorescence assays, its subcellular distribution was investigated by transiently expressing aciculin–GFP in skeletal muscle cells. Aciculin–GFP localized to Z-discs (Fig. 7D–F) and myotome boundaries, structures that are comparable to mammalian MTJs where myofibrils attach to the membrane (Fig. 7G–I).

Subsequently, aciculin was inactivated by injection of morpholino (MO)-modified antisense oligonucleotides directed against the translational start site into one-cell-stage embryos. When injected with a start-site morpholino (MO-start), 83%±6 of injected embryos (n=190; P<0.0001, mean±s.d.) developed severe cardiac and skeletal myopathy, whereas embryos injected with control morpholino were unaffected (n=150). Injection of an independent morpholino directed against the splice donor site of exon five of *pgm5* (MO-splice) resulted in an identical phenotype (93%±5; n=200; P<0.0001), validating its specificity. Knockdown effectiveness was demonstrated by analysis of *pgm5* mRNA by RT-PCR and sequencing: MO-splice led to inclusion of intron five in the mRNA, disruption of the regular reading frame and introduction of premature translation termination codons, which usually lead to nonsense-mediated decay (Fig. 7N; supplementary material Fig. S3B). Western blot analysis of lysates from 72 hpf control and morpholino-treated embryos indicated not only a strong downregulation of aciculin, but also of α-actinin, myomesin and myosin in aciculin-knockdown embryos (supplementary material Fig. S3C), which is comparable to the aciculin-knockdown effect in the IMM cell line. Skeletal muscle dysfunction was accompanied by reduced voluntary motility at 24 hpf (Fig. 7P–R) and failure to execute a 'flight response' when touch-stimulated at 72 hpf (Fig. 7R; supplementary material Movies 1 and 2). Inspection of aciculin morphants with polarized light revealed a strong reduction of birefringence in the somitic musculature (26%±18; P<0.0001), suggesting disorganization of myofibers or loss of myofibrillar integrity (Fig. 7J–M,O). Indeed, staining aciculin-deficient embryos for F-actin and the Z-disc epitope of titin revealed severely disorganized muscle fibers that had often lost their striated pattern and were no longer attached to somite borders (Fig. 7S–V). Ultrastructural characterization confirmed severe myofilament disorganization: myofibrils were irregularly arranged, contained smaller and misaligned Z-discs (Fig. 7W–Z) and failed to attach to myosepta. These *in vivo* findings highlight the essential role of aciculin in myofibril organization and integrity, and in the connection of myofibers to tendons or tendon-like structures.

DISCUSSION

Aciculin has primarily been investigated as an adhesion protein and cytoskeletal component of cell–matrix and cell–cell contacts in muscle and non-muscle cells (Belkin et al., 1994; Belkin and Burridge, 1994; Belkin and Burridge, 1995a; Belkin and Burridge, 1995b; Belkin and Smalheiser, 1996). Correspondingly, the previously reported interaction partners of aciculin were dystrophin and its non-muscle homolog utrophin

Journal of Cell Science (2014) 127, 3578–3592 doi:10.1242/jcs.152157

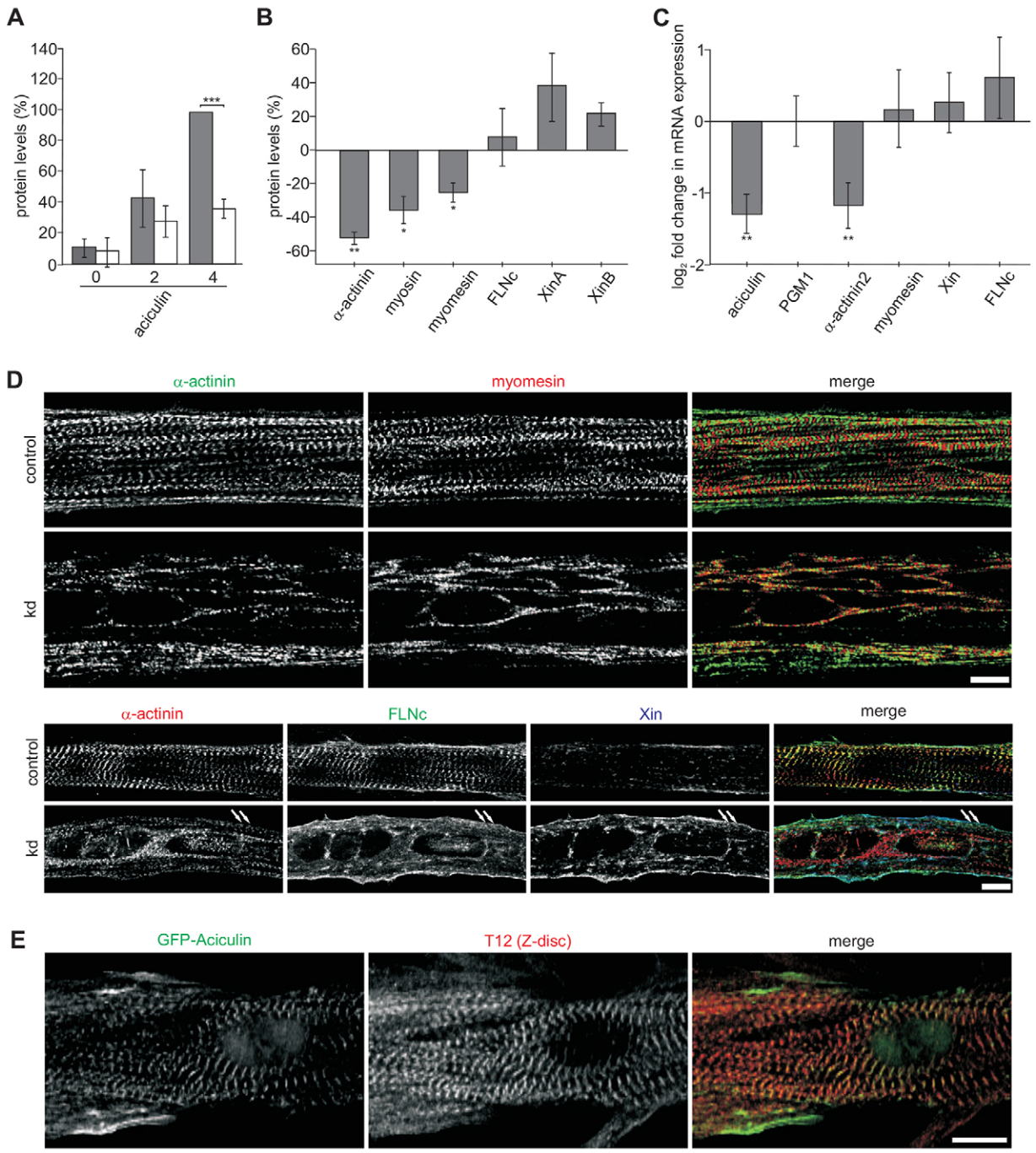

Fig. 6. Aciculin knockdown leads to decreased expression of several myofibrillar proteins and disturbed myofibrillar organization. (A) Aciculin expression in knockdown cells is reduced by ~60%. (B) Quantitative western blotting of aciculin-knockdown cells differentiated for 4 days demonstrated a significant decrease in α-actinin2, myosin heavy chain and myomesin expression, whereas levels of FLNc and Xin were slightly but not significantly increased. (C) Aciculin knockdown leads to reduced levels of α-actinin2-encoding mRNA, whereas no significant changes in expression of other genes were observed. Relative expression levels (log^2 scale) in aciculin knockdown cells compared to control cells are shown normalized to GAPDH. $^{**}P<0.001$; $^{***}P<0.0001$ (Student's *t*-test). Data are means±s.d. of triplicate determinations. Error bars in C represent log_2 values. (D) Control cells differentiated for 6 days show typical myofibrillar localization of α-actinin and FLNc (Z-discs), myomesin (M-bands) and Xin. In aciculin-knockdown cells (kd) this pattern is almost entirely lost, the number of myofibrils is reduced and myofibrils are misaligned. Note that FLNc no longer colocalizes with α-actinin in the few remaining Z-discs of aciculin-knockdown cells (arrows). (E) Transfection of the aciculin-knockdown cells with EGFP-tagged human aciculin leads to rescue of the phenotype. Scale bars: 5 μm.

(Belkin and Burridge, 1995a; Belkin and Burridge, 1995b; Belkin and Smalheiser, 1996). In this study, we show that aciculin is an interaction partner for both Xin and FLNc, not only in adhesion structures but also in premyofibrils and Z-discs. The latter proteins are primarily expressed in striated muscles and are involved in sarcomere development (Eulitz et al., 2013; Sinn et al., 2002; van der Ven et al., 2000a; van der Ven et al., 2000b). Interestingly, they are also particularly associated with areas of

Journal of Cell Science (2014) 127, 3578–3592 doi:10.1242/jcs.152157

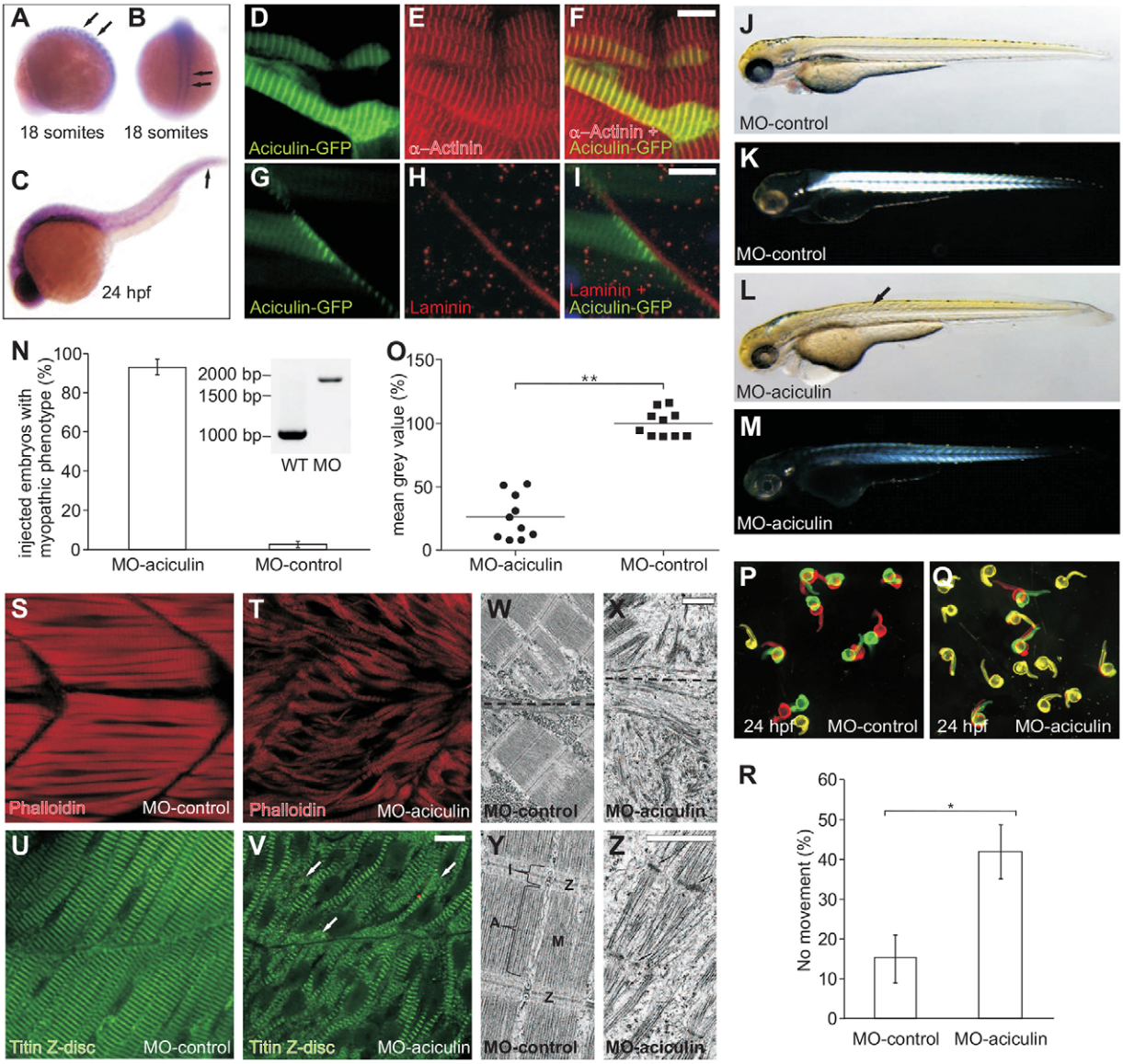

Fig. 7. Knockdown of aciculin leads to myopathy *in vivo*. (A,B) Whole-mount antisense RNA *in situ* hybridization shows strong aciculin expression in the somites of 16-somite-stage embryos (arrows). (C) At 24 hpf, expression is pronounced in developing somites (arrow), the head and the gastrointestinal tract. (D–I) GFP-tagged aciculin (green) colocalizes with α-actinin (red) (D–F) at Z discs and with laminin (red) (G–I) at myosepta. (J–Z) Inactivation of aciculin leads to myopathy. (J,L) Lateral view of MO-control- (J) and MO-aciculin-injected embryos (L) at 72 hpf. Aciculin morphant skeletal muscles appear disorganized (arrow). (N) 93% of embryos injected with MO-aciculin display a myopathic phenotype. Injection of MO-aciculin (MO) leads to abnormal splicing and integration of intron five in the mRNA (product of 1879 bp, see supplementary material Fig. S3) (N, inset). WT, wild-type. Birefringence images of control (K) and MO-aciculin-injected (M) embryos. (O) Quantification of birefringence. Lines represent mean gray values (±s.d., $n=10$). Note that birefringence in skeletal muscles of aciculin morphants is severely reduced. Spontaneous movement assay with false-colored superimposed overviews of embryos at 24 hpf injected with MO-control (P) and MO-aciculin (Q) indicating paralysis of aciculin-deficient individuals. Red pictures, 0 s; green pictures, 10 s. (R) Quantification of ten groups of control and MO-aciculin injected embryos. Results are mean±s.d. for three experiments each including an average of 21 embryos. Note significantly decreased spontaneous movement in aciculin-knockdown individuals. *$P<0.05$; **$P<0.001$ (Student's *t*-test). (S–V) Skeletal muscle of embryos at 72 hpf injected with MO-control (S,U) or MO-aciculin (T,V) and stained with Phalloidin (red, S,T) and for Z-disc titin (green, U,V) showing loss of regular myofiber alignment and in some areas cross-striation (white arrows) in aciculin morphants. Ultrastructure of control embryos (W,Y) shows highly organized sarcomeres with well-aligned thin and thick myofilaments and discernible Z-discs, and A-, I- and M-bands. The somite border is indicated with a dashed line (W,X). MO-aciculin zebrafish (X,Z) show disconnection of myofibrils from the MTJs and loss of orientation and integrity of myofibrils. Arrows indicate Z-body-like structures. Scale bars: 10 μm (D–I, S–V); 1 μm (W–Z).

myofibrillar damage and remodeling (Eulitz et al., 2013; Hawke et al., 2007; Nilsson et al., 2013). Therefore, the interaction of aciculin with these proteins in itself suggests, apart from its essential role in muscle cell attachment, an involvement in assembly, repair and remodeling of the contractile machinery. Indeed, our combined biochemical, biophysical and cell biological evidence supports this dual role both *in vitro* and *in vivo*.

Structural aspects of aciculin interactions

Although aciculin shares considerable sequence similarity with PGM1, suggesting a similar tertiary structure, it lacks enzymatic

Journal of Cell Science (2014) 127, 3578–3592 doi:10.1242/jcs.152157

activity (Belkin et al., 1994). This finding that a modified enzyme might be employed as a stably folding cytoskeletal building block is highly reminiscent of actin, which shares a common ATPase domain with functionally diverse proteins, like hexokinase, Hsp70 and actin-related proteins (Bork et al., 1992; Muller et al., 2005).

Our experiments show that the aciculin regions that are sufficient for binding FLNc and Xin are located at its N- and C-terminus, respectively (Fig. 3F,G), which implies that the opposite ends of aciculin are in close proximity to one another (Dai et al., 1992). This might therefore provoke the observed competition between FLNc and Xin for binding aciculin (Fig. 3D,E). The smallest FLNc fragment that interacts with aciculin is the fragment that contains the four Ig-like domains d18–21. Although the structure of this part of FLNc is unknown, the high level of similarity to FLNa suggests that, in FLNc, interdomain interactions also drive the formation of a similar, compact L-shaped structure (Pentikäinen et al., 2011; Tossavainen et al., 2012). Deletion of a single domain or domain pair brings about a conformational change that hampers the interaction with aciculin. Thus, similar to FLNa, certain ligands will exclusively bind the more compact globularly arranged FLNc C-terminus, whereas others will selectively interact with the stretched molecule in which interdomain interactions are disrupted. Furthermore, the unique insertion in domain 20 is essential for binding because its deletion abolishes the interaction. This also explains why aciculin selectively binds FLNc and not FLNa.

Functional implications of aciculin-containing protein complexes under normal and stress conditions

In addition to these biochemical findings, protein expression and localization data reinforce the functional significance of aciculin-, FLNc- and Xin-containing protein complexes. All three proteins colocalize in junctional structures, premyofibrils and areas of damage and repair, whereas in myofibrillar Z-discs only FLNc and aciculin are represented. Thus, mature Z-discs contain an FLNc–aciculin complex, whereas XinB–FLNc and XinB–aciculin complexes might coexist in junctional areas, premyofibrils and lesions (Fig. 8).

Under conditions of stress, increased XinA quantities are expressed (Chang et al., 2013; Otten et al., 2010). In contrast to XinB, this Xin variant can simultaneously bind FLNc and aciculin (van der Ven et al., 2006), thus enabling the formation of an even more complex ternary protein assembly and integration of further binding partners (Fig. 8). Notably, XinA binds nebulin and nebulette, and might recruit both proteins to premyofibrils and areas of myofibrillar remodeling (Eulitz et al., 2013). At the sarcolemma and in cell–cell and cell–matrix contacts, the presence of XinA enables the formation of protein complexes that might associate simultaneously with many subsarcolemmal proteins, such as dystrophin, γ- and δ-sarcoglycan, β-catenin and ponsin (also known as CAP and SORBS1) (Belkin and Burridge, 1995a; Choi et al., 2007; Thompson et al., 2000; Zhang et al., 2007) (Fig. 8), enhancing the stability of the sarcolemma and its cytoskeleton attachment sites. The significance of these interactions is further highlighted by the pronounced attachment phenotypes of aciculin knockdown described in this work and of FLNc deficiency in mice (Dalkilic et al., 2006) and fish (Fujita et al., 2012; Ruparelia et al., 2012), indicating conservation of protein interactions and functions in all vertebrates from fish to man.

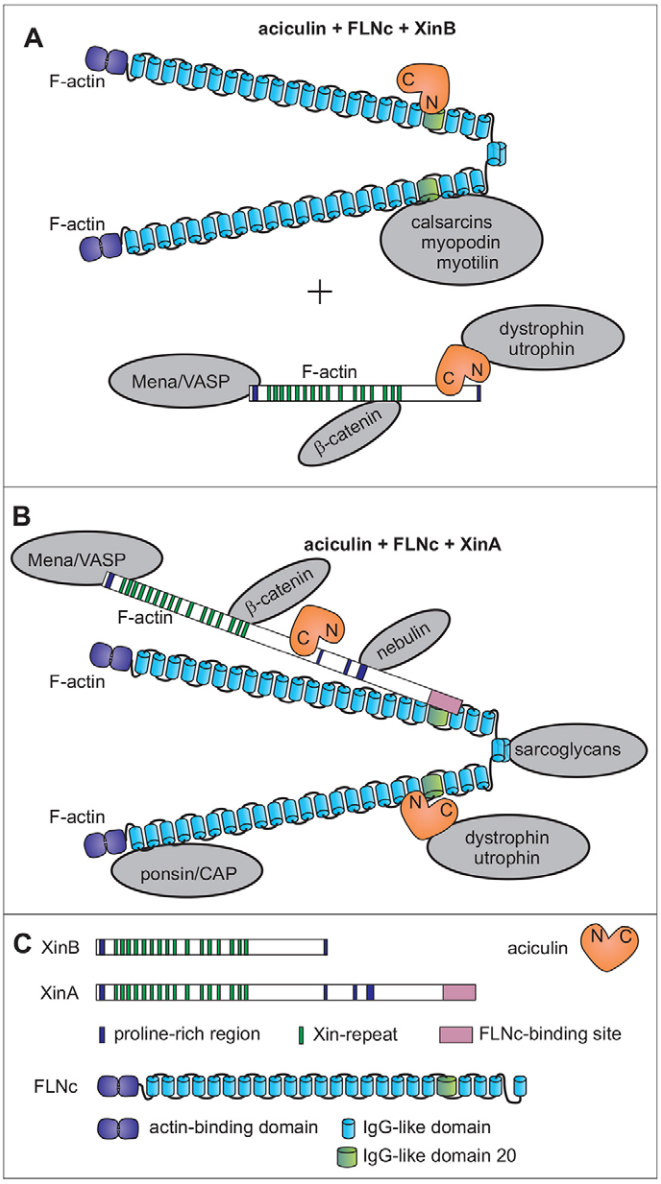

Fig. 8. Hypothetical model of the putative aciculin-containing protein complexes in muscle cells. In the presence of XinB (A), two independent protein complexes would predominate, whereas in the presence of XinA (B) the more extensive ternary protein complex can also be assembled. Proteins and their domains are explained in C.

Subsequently, we aimed to analyze the effect of enhanced contractility in muscle cells on aciculin interactions and turnover. We therefore used EPS to induce contractility in muscle cells and combined it with BiFC and FRAP. To our knowledge this is the first study utilizing a combination of these techniques. Previously, application of EPS has been shown to stimulate sarcomere assembly in C2C12 cells (Fujita et al., 2007; Park et al., 2008) and to trigger various metabolic and transcriptional events typically associated with exercise (Farmawati et al., 2013; Marotta et al., 2004; Nedachi et al., 2008; Nedachi et al., 2009; Wang et al., 2010; Wehrle et al., 1994). Here, we demonstrate that the Xin–aciculin complex, as revealed by BiFC, is localized at FLNc-containing sites during EPS-induced muscle remodeling and seems to be involved in myofibril repair. FRAP of unstimulated myotubes revealed extremely high dynamics and

Journal of Cell Science (2014) 127, 3578–3592 doi:10.1242/jcs.152157

mobility of aciculin compared to other sarcomeric proteins (da Silva Lopes et al., 2011; Hartman et al., 2009; Wang et al., 2005; Wang et al., 2011), both at Z-discs and premyofibrils. Application of EPS even further increased aciculin dynamics (Fig. 4). Similarly, contractility stimulation or application of hormones enhances turnover of CapZ in cardiomyocytes (Hartman et al., 2009; Lin et al., 2013).

Notably, exercise stimulates chaperone-assisted selective autophagy (CASA) (Arndt et al., 2010; Ulbricht et al., 2013). In this work, exercise was induced by EPS. The associated upregulation of BAG3 would result in increased FLN turnover, through its ubiquitylation and subsequent degradation. Given the strong binding affinity between aciculin and FLNc (~51 nM), it is quite likely that the two proteins remain tightly associated and are turned over together by this exercise-stimulated pathway. Therefore exercise-stimulated autophagy might lead to a further increase in the exchange rate of aciculin to ensure stable protein amounts in Z-disc and to prevent damage during exercise. In this context, filamins have been shown to act as mechanosensors (Ehrlicher et al., 2011; Pentikäinen and Ylänne, 2009; Rognoni et al., 2012; Ulbricht et al., 2013), and FLNc probably plays such a role in the Z-disc, at the sarcolemma and in cell–cell and cell–matrix contacts (Ulbricht et al., 2013). FLNc–aciculin binding might be modulated by structural alterations in FLNc, suggesting that aciculin has a role in mechanosensing and signaling during exercise. Taken together, the complexity of protein interactions between aciculin, FLNc and Xin and their further binding partners explains the strong effects of aciculin knockdown on myofibril assembly, maintenance and attachment.

Relative importance of aciculin, FLNc and Xin

The interactions of aciculin with FLNc and Xin raise the question of their relative hierarchical position in the diverse processes involving these proteins, including myofibril development and repair. Xin-deficient mice show a relatively mild phenotype (Otten et al., 2010), and aciculin dynamics and localization is unaffected in cultured myotubes derived from these mice (supplementary material Fig. S1). In contrast, we show here that FLNc localization is aberrant in aciculin-knockdown cells (Fig. 6D). This suggests that the phenotype observed in not only these myotubes, but also in aciculin-deficient zebrafish embryos could be mediated by mislocalization of FLNc. Indeed, FLNc knockdown in cells results primarily in a loss-of-attachment phenotype, whereas FLNc-deficient mice and fish initially form structurally intact, yet functionally impaired, sarcomeres (Dalkilic et al., 2006; Fujita et al., 2012; Ruparelia et al., 2012). Both findings are reminiscent of the cellular aciculin phenotype described here. This suggests that one of the prime tasks of aciculin is to regulate FLNc localization and function. Generally, aciculin seems to be of great importance for muscle differentiation because abrogation of its expression results in a generalized myofibril formation defect as well as reduced expression of multiple myofibrillar proteins. In this respect, it is interesting that, upon knockdown of FLNc in C2C12 cells, a decreased expression of several striated muscle specific proteins is also observed (Dalkilic et al., 2006), highlighting the close functional link between aciculin and FLNc. In contrast, α-actinin expression and localization was not altered upon knockdown of nebulin in primary quail myotubes (Tonino et al., 2010), emphasizing the relative importance of aciculin for muscle development and maintenance.

The different roles of the protein complexes described above during the sequential phases of sarcomere assembly, repair and remodeling remain to be established. Clearly, these proteins extensively colocalize at sites of *de novo* myofibril formation and of remodeling sarcomeres, as well as in regenerating muscle fibers of mdx mice and Duchenne muscular dystrophy patients (A.B., unpublished data). In addition, colocalization of aciculin, together with FLNc and Xin, in aggregates in myofibrillar myopathy patients points to a concerted involvement of Xin, FLNc and aciculin in muscle pathologies (Kley et al., 2013). Finally, aciculin, Xin and FLNc all show increased phosphorylation within 10 min after induced pressure overload mediated by aortic banding of mouse hearts (Chang et al., 2013). All these points support our suggestion that these proteins cooperate in signaling processes involved in adaptation of striated muscle to stress.

Our findings warrant a precise in-depth analysis of these proteins in filaminopathies and other myopathies, and a search for aciculin mutations in myopathy patients. We conclude that besides the known role of aciculin in junctional structures, it has fundamental additional functions in sarcomeric development, stability and remodeling. Which of these functions are administered directly by its multi-adaptor nature, or indirectly through the regulation of FLNc, remains to be investigated.

MATERIALS AND METHODS

Design of cDNA constructs

DNA cloning was performed using standard procedures (Ausubel et al., 1995). The aciculin cDNA sequence was amplified by PCR from a human skeletal muscle cDNA library (BD Biosciences Clontech, Palo Alto, USA), using the primers 5′-TTTACGCGTATGGAGGGGAGC-CCCATCCCG-3′ and 5′-TTTGTCGACGGTGATGACAGTGGGTCCCCT-3′ and cloned into pET23-T7. The N-terminal (amino acids 1–197) and C-terminal (amino acids 380–569) portions of aciculin were cloned in pET23-T7 for pull-down experiments. XinA fragment 903–1200, and XinB and XinB truncation mutants comprising amino acids 1–960, 1–1001 and 1–1057 were cloned in pET23-EEF for co-immunoprecipitation experiments. The FLNc fragment (d18–21) used for pull-down assay was cloned into pGEX6P3 for expression and purification as a GST fusion protein. The same fragments with and without the insertion in d20, d19–20 and d20–21 were cloned in pET23-EEF for co-immunoprecipitation experiments.

Yeast two-hybrid assays

A human Xin cDNA fragment comprising amino acids 756–1119 was cloned into a modified pLex vector and a human heart muscle cDNA library (BD Biosciences Clontech) was screened for interaction partners. Transformation into L40 yeast cells, and culturing and testing for β-galactosidase activity was performed as described previously (van der Ven et al., 2000b).

Bacterial expression constructs, purification of recombinant protein, co-immunoprecipitation and pull-down assay

To biochemically confirm the interaction of aciculin with Xin and FLNc, cDNA fragments and full-length constructs were cloned in pET23-EEF and pET23-T7 (Obermann et al., 1997). Expression and purification of recombinant proteins and co-immunoprecipitation assays were carried out mainly as described previously (Linnemann et al., 2010). For pull-down experiments with FLNc d18–21, FLNc d18–21–GST fusion protein (or GST as negative control) immobilized on glutathione-agarose beads were incubated with the purified N-terminus (amino acids 1–197) and C-terminus (amino acids 380–568) of aciculin under constant agitation at 4℃ for 1 h. Beads were washed with GST-FISH buffer (50 mM Tris-HCl pH 7.4, 100 mM NaCl, 2 mM $MgCl_2$, 10% glycerol and 1% Igepal) and boiled in SDS sample buffer. Bead-associated proteins were separated

by SDS-PAGE, transferred onto nitrocellulose membrane and immunodetected using antibodies directed against the respective tags.

For endogenous co-immunoprecipitation, four-day differentiated C2C12 cells were lysed in sucrose-Tris buffer (0.25 M sucrose, 20 mM $Na_2S_2O_3$, 1 mM β-ME, 50 mM Tris-HCl pH 8.0). The lysate was incubated for 10 min on ice, then sonicated and centrifuged to remove insoluble proteins (16,000 ***g***, 15 min). The supernatant was precleared with Dynabeads Protein G (LifeTechnologies, Darmstadt, Germany) for 1 h at 4℃, and incubated with anti-aciculin antibody or preimmune serum, as a negative control, for 1 h at 4℃ while rotating. Dynabeads were added and the mixture was incubated as described above. Beads were washed three times with PBS plus 0.05% Triton X-100 and boiled in SDS sample buffer. Bead-associated proteins were analyzed as described above.

Cell lysates, SDS-PAGE and western blot analysis

C2C12 cells and immortalized mouse myoblasts (control and aciculin-knockdown cells) at different stages of differentiation were lysed with preheated SDS sample buffer, denatured for 10 min at 95℃ and sonicated. Lysates were adjusted to an identical total protein concentration after quantitative analysis of a Coomassie-stained SDS-polyacrylamide gel. For comparative quantitative blotting, identical total protein amounts were loaded in all lanes. SDS-PAGE was performed as described previously (Laemmli, 1970). Proteins were transferred onto nitrocellulose membranes using a Transblot SD blot apparatus (Biorad, Munich, Germany). Primary antibodies used for immunostaining are described below. Horseradish peroxidase (HRP)- and IRDye 800 CW conjugates were purchased from Jackson ImmunoResearch/Dianova (Hamburg, Germany) and LI-COR Biosciences (Bad Homburg, Germany), respectively. Analysis was performed with a LI-COR Odyssey Classic apparatus, and Odyssey V 3.0 software was used to quantify integrated intensities.

Solid-phase protein-binding assays

Wells of Immulon 2HB microtiter plates (Nunc) were coated overnight with either 2 mg/ml FLNc (d18–21 fragment) or XinB and then blocked with 2% BSA in PBS. Following washing with PBS, the indicated concentrations of aciculin in PBS containing 0.05% Tween-20 were added with or without 0.2 mM or 2 mM of XinB or FLNc (d18–21) and incubated for 2 h at 37℃. Bound aciculin was detected by incubation with 0.2 mg/ml 14F8 antibody for 1 h at 25℃ and HRP-conjugated goat anti-mouse-IgG for 30 min at 25℃. SureBlue TMB (KPL, Gaithersburg, MD) was added and color intensity was measured spectrophotometrically at 450 nm.

Surface plasmon resonance analysis

The interaction of immobilized aciculin with XinB and of immobilized FLNc (d18–21) with aciculin were studied by surface plasmon resonance (SPR) using the BIAcore 3000 biosensor (Biacore AB, Uppsala, Sweden). Covalent immobilization of the proteins (500 response units) on the activated surface of the CM5 sensor chip (GE Healthcare, Pittsburgh, PA) was performed using the amine coupling kit (Biacore AB) as specified by the manufacturer. Binding experiments were performed in HBS-P buffer (10 mM HEPES pH 7.8, containing 150 mM NaCl, 2 mM EDTA and 0.005% surfactant P20) at 10 ml/min flow rate and temperature of 25℃. XinB or aciculin were injected at increasing concentrations using the Application Wizard, and their association and dissociation with immobilized aciculin or FLNc (d18–21) were monitored as a change in SPR response. The chip was regenerated by a 2-min wash with 1 mM urea with 1 mM NaCl. Data were analyzed using BIAevaluation 3.1 software, and by fitting to a pseudo-first-order process also measuring non-specific binding. The maximum change in response units (Rmax) was replotted versus XinB or aciculin concentrations and the data were fitted to a single class of sites by nonlinear regression analysis using SigmaPlot 11 software (Systat Software, San Jose, CA).

Cell culture, transfection and primary mouse myoblast isolation

All media and supplements were from LifeTechnologies. C2C12 cells were grown in proliferation medium [15% FCS, 100 U/ml penicillin, 100 µg/ml streptomycin, 2 mM non-essential amino acids and 1 mM sodium pyruvate, in Dulbecco's modified Eagle's medium (DMEM) with GlutaMAX]. Cells were trypsinized and transfected by nucleofection according to the recommendations of the manufacturer (Lonza, Cologne, Germany). After transfection, cells were seeded on glass coverslips in proliferation medium. Medium was changed 24 h after transfection and cells were differentiated at 90% confluence by changing the medium to differentiation medium (2% horse serum, 100 U/ml penicillin, 100 µg/ml streptomycin, 2 mM non-essential amino-acids and 1 mM sodium pyruvate, in DMEM with GlutaMAX). Cells were allowed to differentiate for up to 7 days. HEK293T cells (ATCC CRL-11268) were grown in proliferation medium (10% FCS, 100 U/ml penicillin, 100 µg/ml streptomycin and 2 mM sodium pyruvate in DMEM with GlutaMAX) at 37℃ under 5% CO_2. Immortalized mouse skeletal myoblasts (IMMs) were isolated and cultured as described previously (Winter et al., 2014). Cells with passage numbers of up to 40 were used for experiments.

Primary myoblasts were isolated from limb muscles from 3-month-old mice deficient for all isoforms of Xin (XinABC$^{-/-}$, *Xirp1*^{tm1Dofr}) (Otten et al., 2010) and wild-type mice (C57BL/6) using a previously published protocol (Yablonka-Reuveni, 2004) with modifications. All mouse experiments were performed according to approved guidelines. Cells were pre-plated on uncoated culture dishes for 2 h and unattached cells were plated on dishes (ibidi, Planegg/Martinsried, Germany) coated with fibronectin (BD Biosciences). At 80% confluency, the medium was changed to transfection medium [73% DBSS-K (116 mM NaCl, 1 mM NaH_2PO_4, 5.5 mM glucose, 32.1 mM $NaHCO_3$), 21% M199, 4% horse serum and 2% L-glutamine], and 4 h later cells were transfected using jetPrime and conditions suggested by the manufacturer (Polyplus, New York, NY). At 24 h after transfection, differentiation was induced by adding differentiation medium as above.

Lentivirus production and transduction of immortalized mouse myoblasts

Lentiviruses were produced by transfection of 70% confluent HEK293T cells with a lentiviral vector containing shRNA against mouse aciculin (MM shRNA V3LMM_443483, ThermoFischer/ABgene, Epsom, UK) or scrambled shRNA, and the packaging plasmids pPAX2 and pMDG, as previously described (Szulc et al., 2006). The medium was changed 6–10 h after transfection, and lentiviral particles containing medium were collected 36–48 h later. Cellular debris was removed by centrifugation (780 ***g***, 5 min) and the supernatant was filtered through a 0.2 µm filter unit (Schleicher-Schuell, Munich, Germany). Lentiviral particles were concentrated by ultracentrifugation for 2 h at 85,000 ***g*** (Beckman SW40Ti rotor) and resuspension of the pellet in 50–100 µl PBS.

Immortalized mouse myoblasts were transduced with lentiviruses at ~30–40% confluence. At 24–48 h post-transduction, the medium was changed to proliferation medium supplemented with 2 µg/ml puromycin (Sigma) to select stably transduced cells. Selected cells were either differentiated for up to 4 days on collagen-coated Petri dishes for protein extraction or for up to 7 days on laminin-coated glass coverslips for immunolocalization studies.

Bimolecular fluorescence complementation

BiFC (Hu et al., 2002) was used to visualize protein interactions in living cells. The vectors enabling expression of Venus1 and Venus2 fusion proteins were as described previously (Eulitz et al., 2013). For the interaction assays, C2C12 cells were transfected with Venus2C–HA–aciculin (aciculin fused with its N-terminus to amino acids 155–238 of the yellow fluorescent protein Venus; linker, RSMGYPYDVPDYAEFTR) and FLAG–XinB–Venus1N (XinB fused with its C-terminus to amino acids 1–154 of Venus; linker, VDGTAGPGS). All proteins were also transfected as Venus fusion proteins and co-transfected with the compatible non-fluorescent Venus fragments alone in order to evaluate potential unspecific BiFC complex formation. Cells were allowed to differentiate and, afterwards, were fixed, stained and analyzed with a confocal laser scanning microscope equipped with a CO_2 chamber (LSM710; Carl Zeiss, Jena, Germany) or a spinning disc microscope (Cell Observer SD; Carl Zeiss).

Fluorescence recovery after photobleaching and data analysis

Cells were transfected with EGFP–aciculin and seeded on Fluorodish glass-bottom dishes (WPI, Berlin, Germany). FRAP experiments were performed after 7 days of differentiation using the LSM710 confocal laser-scanning microscope. Cells were kept at 37℃ under 5% CO_2. Zen 2009 software (Carl Zeiss) was used for image processing. The region of interest (ROI) for bleaching was limited to a single Z-disc or a non-striated premyofibril. Photobleaching was done with 100% intensity of the 405-nm laser. A series of three images was taken before bleaching and, immediately after photobleaching, images were taken every second until the signal fully recovered (250–300 s). Normalized FRAP curves were generated from raw data as previously described (Al Tanoury et al., 2010). FRAP data are presented as the mean of four or five individual experiments. For photobleaching upon inhibition of contraction, 1 mM BDM (Sigma) was added to the culture medium 30 min before starting the experiments. Cells were kept in this medium throughout the analysis.

Electrical pulse stimulation

For FRAP mobility assays, myotubes developed from transfected C2C12 cells or primary mouse myoblasts on glass-bottom dishes were electrically stimulated by home-made 1-mm-thick carbon electrodes, 2 cm apart, by applying pulses of 10 V for 10 ms at a frequency of 1 Hz using a C-Pace unit (Ion Optix, Milton, MA). Cells were analyzed as described above. For exercise assays, differentiated C2C12 myotubes on uncoated glass coverslips were placed in six-well dishes, and were electrically stimulated using a six-well C-dish (Ion Optix) and a C-Pace unit using identical settings, for a total time of 5 h. Cells were fixed and stained as described below.

Antibodies and immunostaining

The mouse monoclonal antibodies (mAbs) XR1, recognizing XinA and XinB (van der Ven et al., 2006), T12, which labels a titin epitope close to the Z-disc (Fürst et al., 1988), RR90, recognizing FLNa and FLNc (van der Ven et al., 2000a), 14F8, recognizing aciculin (Belkin et al., 1994), and BB78, recognizing myomesin (Vinkemeier et al., 1993) have been described previously. Anti-GAPDH (5C6) was purchased from Merck Millipore (Darmstadt, Germany). Anti-laminin (Lam-89) and anti-α-actinin (EA-53) were from Sigma (Taufkirchen, Germany). The rabbit serum against sarcomeric α-actinin (RaA653) has been described previously (van der Ven et al., 2000a). The mAb against the T7 tag was purchased from Novagen (Heidelberg, Germany). The rat mAb YL1/2 was raised against the C-terminus of tyrosinated tubulin and recognizes the C-terminal GluGluPhe (EEF) tag (Wehland et al., 1983). Antibodies against HA and FLAG tags were from Roche Applied Science (Mannheim, Germany) and Sigma, respectively. Novel polyclonal rabbit antisera were raised against recombinantly expressed aciculin and FLNc Ig-like domains 16–20 (BioGenes, Berlin, Germany). The former serum was preabsorbed against PGM1 to avoid cross-reactivity. Secondary antibodies conjugated to Alexa Fluor 594, DyLight488, Cy3 and Cy5 were purchased from Jackson ImmunoResearch/Dianova (Hamburg, Germany).

Cells were fixed in a 1:1 mixture of methanol and acetone for 5 min at −20℃. Frozen tissue sections were fixed with methanol (2 min, −20℃) and acetone (20 s, −20℃). After washing with PBS, cells and sections were blocked with 10% normal goat serum with 1% BSA in PBS for 30 min. Primary antibodies diluted in 1% BSA in PBS were applied for 1–16 h. After washing with PBS, specimens were incubated with secondary antibodies diluted in 1% BSA in PBS, washed with PBS and mounted in Mowiol containing 10% N-propyl gallate. Cells were analyzed and photographed using a Zeiss LSM710 confocal microscope.

Zebrafish methods

Care and breeding, as well as injection procedures, of zebrafish (*Danio rerio*) were as described previously (Just et al., 2011a). If not indicated otherwise, the splice-site-targeting morpholino against aciculin (32 ng, 5′-ATGAGATAAGAGGCAAGCACCCCAT-3′) was applied. The phenotype was phenocopied by the start-site-targeting morpholino (16 ng, 5′-AAATGGGTATAGGGTTTGTCTCCAT-3′). Morpholinos were from Gene Tools (Philomath, OR). The present study was performed after securing appropriate institutional approvals that conforms to the Guide for the Care and Use of Laboratory Animals published by the 'US National Institutes of Health' (NIH Publication No. 85–23, revised 1996).

Whole-mount *in situ* hybridization was carried out essentially as described previously (Thisse and Thisse, 2008) using a 592-bp antisense probe, forward primer 5′-TGGGTGAGAATGGGTTTTTC-3, and reverse primer 5′-GATCCTTAGGCCCTGTTTCC-3′. Immunostaining of zebrafish embryos was carried out as described previously (Inoue and Wittbrodt, 2011). Full-length zebrafish aciculin cDNA was PCR-amplified using primers 5′-ATGGAGACAAACCCTATACCCA-3′ and 5′-GGTGATGATATTAGGCCCTCTG-3′, cloned into the Tol2 vector system (Kwan et al., 2007) and fused with GFP. Aciculin–GFP was expressed under the striated-muscle-specific unc45 promoter (Roostalu and Strähle, 2012). The vector was injected into one-cell-stage fertilized embryos at 25 ng/µl. For birefringence assays, zebrafish larvae were anesthetized with tricaine and embedded in tissue tec. Pictures were acquired between two polarizing filters on an Olympus SZX16 with a DP72 camera and the Olympus Stream software (Olympus, Hamburg, Germany). ISO was fixed to 400 and exposure time to 296 ms. Data analysis was carried out as described previously (Charvet et al., 2013). Electron micrographs were obtained essentially as described previously (Just et al., 2011b). To measure movement of the zebrafish embryos, images showing several larvae at 24 hpf were acquired; at least four pictures were taken, each 10 s apart. Two subsequent pictures were false-colored and superimposed. The number of moving larvae was counted and for each series the mean was calculated as one data point.

Acknowledgements

We thank Karin Bois and Corina Mirschkorsch (Institute for Cell Biology, Bonn, Germany) for technical assistance.

Competing interests

The authors declare no competing interests.

Author contributions

S.M., J.B.B., S.Y., P.S., L.W. performed experiments and analyzed data; G.W., W.R., Z.O. and G.K. provided expertise and helped in designing the experiments; P.F.M.v.d.V., S.J., A.M.B. and D.O.F. designed experiments and wrote the manuscript. All authors contributed to writing and correcting the manuscript.

Funding

This work was supported by the German Research Foundation FOR1228 to D.O.F. [grant number Fu339/7], W.R. [grant number RO2173/4] and S.J. [grant number JU2859/1], and FOR1352 to D.O.F. [grant number Fu339/9]; the Austrian Science Research Fund (FWF) [grant number I413-B09, part of the Multilocation DFG-Research Unit 1228; to G.W.]; and the Seventh Framework Programme for Research and Technological Development of the EU (MUZIC) to D.O.F. Work in A.M.B. laboratory was supported by funds from the University of Maryland School of Medicine.

Supplementary material

Supplementary material available online at
http://jcs.biologists.org/lookup/suppl/doi:10.1242/jcs.152157/-/DC1

References

Al Tanoury, Z., Schaffner-Reckinger, E., Halavatyi, A., Hoffmann, C., Moes, M., Hadzic, E., Catillon, M., Yatskou, M. and Friederich, E. (2010). Quantitative kinetic study of the actin-bundling protein L-plastin and of its impact on actin turn-over. *PLoS ONE* **5**, e9210.

Arndt, V., Dick, N., Tawo, R., Dreiseidler, M., Wenzel, D., Hesse, M., Fürst, D. O., Saftig, P., Saint, R., Fleischmann, B. K. et al. (2010). Chaperone-assisted selective autophagy is essential for muscle maintenance. *Curr. Biol.* **20**, 143-148.

Ausubel, F. M., Brent, R., Kingston, R. E., Moore, D. D., Seidman, J. G., Smith, J. A. and Struhl, K. (1995). *Short Protocols in Molecular Biology*. New York, NY: Wiley and Sons, Inc.

Belkin, A. M. and Burridge, K. (1994). Expression and localization of the phosphoglucomutase-related cytoskeletal protein, aciculin, in skeletal muscle. *J. Cell Sci.* **107**, 1993-2003.

Belkin, A. M. and Burridge, K. (1995a). Association of aciculin with dystrophin and utrophin. *J. Biol. Chem.* **270**, 6328-6337.

Belkin, A. M. and Burridge, K. (1995b). Localization of utrophin and aciculin at sites of cell-matrix and cell-cell adhesion in cultured cells. *Exp. Cell Res.* **221**, 132-140.
Belkin, A. M. and Smalheiser, N. R. (1996). Localization of cranin (dystroglycan) at sites of cell-matrix and cell-cell contact: recruitment to focal adhesions is dependent upon extracellular ligands. *Cell Adhes. Commun.* **4**, 281-296.
Belkin, A. M., Klimanskaya, I. V., Lukashev, M. E., Lilley, K., Critchley, D. R. and Koteliansky, V. E. (1994). A novel phosphoglucomutase-related protein is concentrated in adherens junctions of muscle and nonmuscle cells. *J. Cell Sci.* **107**, 159-173.
Bönnemann, C. G., Thompson, T. G., van der Ven, P. F. M., Goebel, H. H., Warlo, I., Vollmers, B., Reimann, J., Herms, J., Gautel, M., Takada, F. et al. (2003). Filamin C accumulation is a strong but nonspecific immunohistochemical marker of core formation in muscle. *J. Neurol. Sci.* **206**, 71-78.
Bork, P., Sander, C. and Valencia, A. (1992). An ATPase domain common to prokaryotic cell cycle proteins, sugar kinases, actin, and hsp70 heat shock proteins. *Proc. Natl. Acad. Sci. USA* **89**, 7290-7294.
Chang, Y. W., Chang, Y. T., Wang, Q., Lin, J. J., Chen, Y. J. and Chen, C. C. (2013). Quantitative phosphoproteomic study of pressure-overloaded mouse heart reveals dynamin-related protein 1 as a modulator of cardiac hypertrophy. *Mol. Cell. Proteomics* **12**, 3094-3107.
Charvet, B., Guiraud, A., Malbouyres, M., Zwolanek, D., Guillon, E., Bretaud, S., Monnot, C., Schulze, J., Bader, H. L., Allard, B. et al. (2013). Knockdown of col22a1 gene in zebrafish induces a muscular dystrophy by disruption of the myotendinous junction. *Development* **140**, 4602-4613.
Cherepanova, O., Orlova, A., Galkin, V. E., van der Ven, P. F. M., Fürst, D. O., Jin, J. P. and Egelman, E. H. (2006). Xin-repeats and nebulin-like repeats bind to F-actin in a similar manner. *J. Mol. Biol.* **356**, 714-723.
Choi, S., Gustafson-Wagner, E. A., Wang, Q., Harlan, S. M., Sinn, H. W., Lin, J. L. and Lin, J. J. (2007). The intercalated disk protein, mXinalpha, is capable of interacting with β-catenin and bundling actin filaments [corrected]. *J. Biol. Chem.* **282**, 36024-36036.
da Silva Lopes, K., Pietas, A., Radke, M. H. and Gotthardt, M. (2011). Titin visualization in real time reveals an unexpected level of mobility within and between sarcomeres. *J. Cell Biol.* **193**, 785-798.
Dai, J. B., Liu, Y., Ray, W. J., Jr and Konno, M. (1992). The crystal structure of muscle phosphoglucomutase refined at 2.7-angstrom resolution. *J. Biol. Chem.* **267**, 6322-6337.
Dalkilic, I., Schienda, J., Thompson, T. G. and Kunkel, L. M. (2006). Loss of FilaminC (FLNc) results in severe defects in myogenesis and myotube structure. *Mol. Cell. Biol.* **26**, 6522-6534.
Ehrlicher, A. J., Nakamura, F., Hartwig, J. H., Weitz, D. A. and Stossel, T. P. (2011). Mechanical strain in actin networks regulates FilGAP and integrin binding to filamin A. *Nature* **478**, 260-263.
Eulitz, S., Sauer, F., Pelissier, M. C., Boisguerin, P., Molt, S., Schuld, J., Orfanos, Z., Kley, R. A., Volkmer, R., Wilmanns, M. et al. (2013). Identification of Xin-repeat proteins as novel ligands of the SH3 domains of nebulin and nebulette and analysis of their interaction during myofibril formation and remodeling. *Mol. Biol. Cell* **24**, 3215-3226.
Farmawati, A., Kitajima, Y., Nedachi, T., Sato, M., Kanzaki, M. and Nagatomi, R. (2013). Characterization of contraction-induced IL-6 up-regulation using contractile C2C12 myotubes. *Endocr. J.* **60**, 137-147.
Feng, H. Z., Wang, Q., Reiter, R. S., Lin, J. L., Lin, J. J. and Jin, J. P. (2013). Localization and function of Xinα in mouse skeletal muscle. *Am. J. Physiol.* **304**, C1002-C1012.
Fujita, H., Nedachi, T. and Kanzaki, M. (2007). Accelerated de novo sarcomere assembly by electric pulse stimulation in C2C12 myotubes. *Exp. Cell Res.* **313**, 1853-1865.
Fujita, M., Mitsuhashi, H., Isogai, S., Nakata, T., Kawakami, A., Nonaka, I., Noguchi, S., Hayashi, Y. K., Nishino, I. and Kudo, A. (2012). Filamin C plays an essential role in the maintenance of the structural integrity of cardiac and skeletal muscles, revealed by the medaka mutant zacro. *Dev. Biol.* **361**, 79-89.
Fürst, D. O., Osborn, M., Nave, R. and Weber, K. (1988). The organization of titin filaments in the half-sarcomere revealed by monoclonal antibodies in immunoelectron microscopy: a map of ten nonrepetitive epitopes starting at the Z line extends close to the M line. *J. Cell Biol.* **106**, 1563-1572.
Gustafson-Wagner, E. A., Sinn, H. W., Chen, Y. L., Wang, D. Z., Reiter, R. S., Lin, J. L., Yang, B., Williamson, R. A., Chen, J., Lin, C. I. et al. (2007). Loss of mXinalpha, an intercalated disk protein, results in cardiac hypertrophy and cardiomyopathy with conduction defects. *Am. J. Physiol.* **293**, H2680-H2692.
Hartman, T. J., Martin, J. L., Solaro, R. J., Samarel, A. M. and Russell, B. (2009). CapZ dynamics are altered by endothelin-1 and phenylephrine via PIP2- and PKC-dependent mechanisms. *Am. J. Physiol.* **296**, C1034-C1039.
Hawke, T. J., Atkinson, D. J., Kanatous, S. B., Van der Ven, P. F. M., Goetsch, S. C. and Garry, D. J. (2007). Xin, an actin binding protein, is expressed within muscle satellite cells and newly regenerated skeletal muscle fibers. *Am. J. Physiol.* **293**, C1636-C1644.
Hu, C. D., Chinenov, Y. and Kerppola, T. K. (2002). Visualization of interactions among bZIP and Rel family proteins in living cells using bimolecular fluorescence complementation. *Mol. Cell* **9**, 789-798.
Inoue, D. and Wittbrodt, J. (2011). One for all – a highly efficient and versatile method for fluorescent immunostaining in fish embryos. *PLoS ONE* **6**, e19713.
Just, S., Berger, I. M., Meder, B., Backs, J., Keller, A., Marquart, S., Frese, K., Patzel, E., Rauch, G. J., Katus, H. A. et al.; Tübingen 2000 Screen Consortium (2011a). Protein kinase D2 controls cardiac valve formation in zebrafish by regulating histone deacetylase 5 activity. *Circulation* **124**, 324-334.
Just, S., Meder, B., Berger, I. M., Etard, C., Trano, N., Patzel, E., Hassel, D., Marquart, S., Dahme, T., Vogel, B. et al. (2011b). The myosin-interacting protein SMYD1 is essential for sarcomere organization. *J. Cell Sci.* **124**, 3127-3136.
Kley, R. A., Maerkens, A., Leber, Y., Theis, V., Schreiner, A., van der Ven, P. F. M., Uszkoreit, J., Stephan, C., Eulitz, S., Euler, N. et al. (2013). A combined laser microdissection and mass spectrometry approach reveals new disease relevant proteins accumulating in aggregates of filaminopathy patients. *Mol. Cell. Proteomics* **12**, 215-227.
Koteliansky, V. E., Belkin, A. M., Ornatsky, O. I., Vasilevskaya, T. D. and Glukhova, M. A. (1989). Identification and immunolocalization of a new component of human cardiac muscle intercalated disc. *J. Mol. Cell. Cardiol.* **21** Suppl. 1:, 23-29.
Kwan, K. M., Fujimoto, E., Grabher, C., Mangum, B. D., Hardy, M. E., Campbell, D. S., Parant, J. M., Yost, H. J., Kanki, J. P. and Chien, C. B. (2007). The Tol2kit: a multisite gateway-based construction kit for Tol2 transposon transgenesis constructs. *Dev. Dyn.* **236**, 3088-3099.
Laemmli, U. K. (1970). Cleavage of structural proteins during the assembly of the head of bacteriophage T4. *Nature* **227**, 680-685.
Lin, Y. H., Li, J., Swanson, E. R. and Russell, B. (2013). CapZ and actin capping dynamics increase in myocytes after a bout of exercise and abates in hours after stimulation ends. *J. Appl. Physiol.* **114**, 1603-1609.
Linnemann, A., van der Ven, P. F. M., Vakeel, P., Albinus, B., Simonis, D., Bendas, G., Schenk, J. A., Micheel, B., Kley, R. A. and Fürst, D. O. (2010). The sarcomeric Z-disc component myopodin is a multiadapter protein that interacts with filamin and alpha-actinin. *Eur. J. Cell Biol.* **89**, 681-692.
Marotta, M., Bragós, R. and Gómez-Foix, A. M. (2004). Design and performance of an electrical stimulator for long-term contraction of cultured muscle cells. *Biotechniques* **36**, 68-73.
Moiseeva, E. P., Belkin, A. M., Spurr, N. K., Koteliansky, V. E. and Critchley, D. R. (1996). A novel dystrophin/utrophin-associated protein is an enzymatically inactive member of the phosphoglucomutase superfamily. *Eur. J. Biochem.* **235**, 103-113.
Morgan, J. E., Beauchamp, J. R., Pagel, C. N., Peckham, M., Ataliotis, P., Jat, P. S., Noble, M. D., Farmer, K. and Partridge, T. A. (1994). Myogenic cell lines derived from transgenic mice carrying a thermolabile T antigen: a model system for the derivation of tissue-specific and mutation-specific cell lines. *Dev. Biol.* **162**, 486-498.
Muller, J., Oma, Y., Vallar, L., Friederich, E., Poch, O. and Winsor, B. (2005). Sequence and comparative genomic analysis of actin-related proteins. *Mol. Biol. Cell* **16**, 5736-5748.
Nedachi, T., Fujita, H. and Kanzaki, M. (2008). Contractile C2C12 myotube model for studying exercise-inducible responses in skeletal muscle. *Am. J. Physiol.* **295**, E1191-E1204.
Nedachi, T., Hatakeyama, H., Kono, T., Sato, M. and Kanzaki, M. (2009). Characterization of contraction-inducible CXC chemokines and their roles in C2C12 myocytes. *Am. J. Physiol.* **297**, E866-E878.
Nilsson, M. I., Nissar, A. A., Al-Sajee, D., Tarnopolsky, M. A., Parise, G., Lach, B., Fürst, D. O., van der Ven, P. F. M., Kley, R. A. and Hawke, T. J. (2013). Xin is a marker of skeletal muscle damage severity in myopathies. *Am. J. Pathol.* **183**, 1703-1709.
Obermann, W. M. J., Gautel, M., Weber, K. and Fürst, D. O. (1997). Molecular structure of the sarcomeric M band: mapping of titin and myosin binding domains in myomesin and the identification of a potential regulatory phosphorylation site in myomesin. *EMBO J.* **16**, 211-220.
Otten, J., van der Ven, P. F. M., Vakeel, P., Eulitz, S., Kirfel, G., Brandau, O., Boesl, M., Schrickel, J. W., Linhart, M., Hayess, K. et al. (2010). Complete loss of murine Xin results in a mild cardiac phenotype with altered distribution of intercalated discs. *Cardiovasc. Res.* **85**, 739-750.
Otten, C., van der Ven, P. F. M., Lewrenz, I., Paul, S., Steinhagen, A., Busch-Nentwich, E., Eichhorst, J., Wiesner, B., Stemple, D., Strähle, U. et al. (2012). Xirp proteins mark injured skeletal muscle in zebrafish. *PLoS ONE* **7**, e31041.
Pacholsky, D., Vakeel, P., Himmel, M., Löwe, T., Stradal, T., Rottner, K., Fürst, D. O. and van der Ven, P. F. M. (2004). Xin repeats define a novel actin-binding motif. *J. Cell Sci.* **117**, 5257-5268.
Park, H., Bhalla, R., Saigal, R., Radisic, M., Watson, N., Langer, R. and Vunjak-Novakovic, G. (2008). Effects of electrical stimulation in C2C12 muscle constructs. *J. Tissue Eng. Regen. Med.* **2**, 279-287.
Pentikäinen, U. and Ylänne, J. (2009). The regulation mechanism for the auto-inhibition of binding of human filamin A to integrin. *J. Mol. Biol.* **393**, 644-657.
Pentikäinen, U., Jiang, P., Takala, H., Ruskamo, S., Campbell, I. D. and Ylänne, J. (2011). Assembly of a filamin four-domain fragment and the influence of splicing variant-1 on the structure. *J. Biol. Chem.* **286**, 26921-26930.
Rezvani, M., Ornatsky, O. I., Connor, M. K., Eisenberg, H. A. and Hood, D. A. (1996). Dystrophin, vinculin, and aciculin in skeletal muscle subject to chronic use and disuse. *Med. Sci. Sports Exerc.* **28**, 79-84.
Rognoni, L., Stigler, J., Pelz, B., Ylänne, J. and Rief, M. (2012). Dynamic force sensing of filamin revealed in single-molecule experiments. *Proc. Natl. Acad. Sci. USA* **109**, 19679-19684.
Roostalu, U. and Strähle, U. (2012). In vivo imaging of molecular interactions at damaged sarcolemma. *Dev. Cell* **22**, 515-529.

Ruparelia, A. A., Zhao, M., Currie, P. D. and Bryson-Richardson, R. J. (2012). Characterization and investigation of zebrafish models of filamin-related myofibrillar myopathy. *Hum. Mol. Genet.* **21**, 4073-4083.
Sewry, C. A., Müller, C., Davis, M., Dwyer, J. S., Dove, J., Evans, G., Schröder, R., Fürst, D., Helliwell, T., Laing, N. et al. (2002). The spectrum of pathology in central core disease. *Neuromuscul. Disord.* **12**, 930-938.
Sinn, H. W., Balsamo, J., Lilien, J. and Lin, J. J. (2002). Localization of the novel Xin protein to the adherens junction complex in cardiac and skeletal muscle during development. *Dev. Dyn.* **225**, 1-13.
Szulc, J., Wiznerowicz, M., Sauvain, M. O., Trono, D. and Aebischer, P. (2006). A versatile tool for conditional gene expression and knockdown. *Nat. Methods* **3**, 109-116.
Thisse, C. and Thisse, B. (2008). High-resolution in situ hybridization to whole-mount zebrafish embryos. *Nat. Protoc.* **3**, 59-69.
Thompson, T. G., Chan, Y. M., Hack, A. A., Brosius, M., Rajala, M., Lidov, H. G., McNally, E. M., Watkins, S. and Kunkel, L. M. (2000). Filamin 2 (FLN2): A muscle-specific sarcoglycan interacting protein. *J. Cell Biol.* **148**, 115-126.
Tonino, P., Pappas, C. T., Hudson, B. D., Labeit, S., Gregorio, C. C. and Granzier, H. (2010). Reduced myofibrillar connectivity and increased Z-disk width in nebulin-deficient skeletal muscle. *J. Cell Sci.* **123**, 384-391.
Tossavainen, H., Koskela, O., Jiang, P., Ylänne, J., Campbell, I. D., Kilpeläinen, I. and Permi, P. (2012). Model of a six immunoglobulin-like domain fragment of filamin A (16-21) built using residual dipolar couplings. *J. Am. Chem. Soc.* **134**, 6660-6672.
Ulbricht, A., Eppler, F. J., Tapia, V. E., van der Ven, P. F. M., Hampe, N., Hersch, N., Vakeel, P., Stadel, D., Haas, A., Saftig, P. et al. (2013). Cellular mechanotransduction relies on tension-induced and chaperone-assisted autophagy. *Curr. Biol.* **23**, 430-435.
van der Ven, P. F. M., Obermann, W. M. J., Lemke, B., Gautel, M., Weber, K. and Fürst, D. O. (2000a). Characterization of muscle filamin isoforms suggests a possible role of γ-filamin/ABP-L in sarcomeric Z-disc formation. *Cell Motil. Cytoskeleton* **45**, 149-162.
van der Ven, P. F. M., Wiesner, S., Salmikangas, P., Auerbach, D., Himmel, M., Kempa, S., Hayess, K., Pacholsky, D., Taivainen, A., Schröder, R. et al. (2000b). Indications for a novel muscular dystrophy pathway. γ-filamin, the muscle-specific filamin isoform, interacts with myotilin. *J. Cell Biol.* **151**, 235-248.
van der Ven, P. F. M., Ehler, E., Vakeel, P., Eulitz, S., Schenk, J. A., Milting, H., Micheel, B. and Fürst, D. O. (2006). Unusual splicing events result in distinct Xin isoforms that associate differentially with filamin c and Mena/VASP. *Exp. Cell Res.* **312**, 2154-2167.
Vinkemeier, U., Obermann, W., Weber, K. and Fürst, D. O. (1993). The globular head domain of titin extends into the center of the sarcomeric M band. cDNA cloning, epitope mapping and immunoelectron microscopy of two titin-associated proteins. *J. Cell Sci.* **106**, 319-330.
Wang, D. Z., Reiter, R. S., Lin, J. L., Wang, Q., Williams, H. S., Krob, S. L., Schultheiss, T. M., Evans, S. and Lin, J. J. (1999). Requirement of a novel gene, Xin, in cardiac morphogenesis. *Development* **126**, 1281-1294.
Wang, J., Shaner, N., Mittal, B., Zhou, Q., Chen, J., Sanger, J. M. and Sanger, J. W. (2005). Dynamics of Z-band based proteins in developing skeletal muscle cells. *Cell Motil. Cytoskeleton* **61**, 34-48.
Wang, Y., Zhao, Z., Li, Y., Li, Y., Wu, J., Fan, X. and Yang, P. (2010). Up-regulated alpha-actin expression is associated with cell adhesion ability in 3-D cultured myocytes subjected to mechanical stimulation. *Mol. Cell. Biochem.* **338**, 175-181.
Wang, J., Dube, D. K., Mittal, B., Sanger, J. M. and Sanger, J. W. (2011). Myotilin dynamics in cardiac and skeletal muscle cells. *Cytoskeleton* **68**, 661-670.
Wehland, J., Willingham, M. C. and Sandoval, I. V. (1983). A rat monoclonal antibody reacting specifically with the tyrosylated form of α-tubulin. I. Biochemical characterization, effects on microtubule polymerization in vitro, and microtubule polymerization and organization in vivo. *J. Cell Biol.* **97**, 1467-1475.
Wehrle, U., Düsterhöft, S. and Pette, D. (1994). Effects of chronic electrical stimulation on myosin heavy chain expression in satellite cell cultures derived from rat muscles of different fiber-type composition. *Differentiation* **58**, 37-46.
Winter, L., Staszewska, I., Mihailovska, E., Fischer, I., Goldmann, W. H., Schröder, R. and Wiche, G. (2014). Ameliorating pathological protein-aggregation in plectin-deficient muscle through a chemical chaperone. *J. Clin. Invest.* **124**, 1144-1157.
Yablonka-Reuveni, Z. (2004). Isolation and culture of myogenic stem cells. In *Handbook of Stem Cells: Adult and Fetal Stem Cells,* Vol. 2 (ed. R. Lanza, H. Blau, D. Melton, M. Moore, E. D. Thomas, C. Verfaillie, I. Weissman and M. West), pp. 571-580. San Diego, CA: Elsevier Academic Press.
Yu, J. G. and Thornell, L. E. (2002). Desmin and actin alterations in human muscles affected by delayed onset muscle soreness: a high resolution immunocytochemical study. *Histochem. Cell Biol.* **118**, 171-179.
Yu, J. G., Carlsson, L. and Thornell, L. E. (2004). Evidence for myofibril remodeling as opposed to myofibril damage in human muscles with DOMS: an ultrastructural and immunoelectron microscopic study. *Histochem. Cell Biol.* **121**, 219-227.
Zhang, M., Liu, J., Cheng, A., Deyoung, S. M. and Saltiel, A. R. (2007). Identification of CAP as a costameric protein that interacts with filamin C. *Mol. Biol. Cell* **18**, 4731-4740.